

**Electronic Supplementary Information for:**

**Ultrafast excited-state relaxation of a binuclear Ag(I) phosphine complex in gas phase and solution**

S. V. Kruppa<sup>1,a)</sup>, F. Bäppler<sup>2,a)</sup>, W. Klopper<sup>3</sup>, S. P. Walg<sup>4</sup>, W. R. Thiel<sup>1</sup>, R. Diller<sup>2,b)</sup>, C. Riehn<sup>1,5,b)</sup>

<sup>1</sup>Department of Chemistry, TU Kaiserslautern, Erwin-Schrödinger-Str. 52, D-67663 Kaiserslautern, Germany.

<sup>2</sup>Department of Physics, TU Kaiserslautern, Erwin-Schrödinger-Str. 46, D-67663 Kaiserslautern, Germany.

<sup>3</sup>Karlsruhe Institute of Technology (KIT), Institute of Physical Chemistry, Fritz-Haber-Weg 2, D-76131 Karlsruhe, Germany.

<sup>4</sup>Institute of Chemistry, Inorganic Chemistry, University of Graz, Schubert-Str. 1, 8010 Graz, Austria.

<sup>5</sup>Forschungszentrum OPTIMAS, Erwin-Schrödinger-Str. 46, D-67663 Kaiserslautern, Germany.

---

<sup>a)</sup> S. V. Kruppa and F. Bäppler contributed equally to this work.

<sup>b)</sup> Corresponding authors: diller@physik.uni-kl.de, riehn@chemie.uni-kl.de.

## Table of Contents

- Fig. S1** Absorption and luminescence spectra of  $[\text{Ag}_2(\text{dcpm})_2](\text{PF}_6)_2$  in MeCN and MeOH.
- Fig. S2** Luminescence excitation spectrum of  $[\text{Ag}_2(\text{dcpm})_2](\text{PF}_6)_2$  in MeCN.
- Figs. S3,S4**  $^{31}\text{P}$ -NMR spectrum of  $[\text{Ag}_2(\text{dcpm})_2](\text{PF}_6)_2$  in MeCN-d3 and MeOD-d4.
- Fig. S5** ESI-MS of  $[\text{Ag}_2(\text{dcpm})_2](\text{PF}_6)_2$  (MeCN solution).
- Fig. S6** Spectral profiles of nonlinear frequency converters (TOPAS-C, Light Conversion).
- Fig. S7** UV-PD yield spectrum of  $[\text{Ag}_2(\text{dcpm})_2]^{2+}$  and transmittance of fused silica window.
- Fig. S8** Channel specific energy dependence of the PD yield for  $[\text{Ag}_2(\text{dcpm})_2]^{2+}$  at 263nm.
- Fig. S9** Energy dependent UV-PD yield spectra of  $[\text{Ag}_2(\text{dcpm})_2]^{2+}$  (at 0.4, 1.2 and 2.0  $\mu\text{J}$ ).
- Figs. S10-S12** Channel specific PD yield dependence on irradiation time for  $[\text{Ag}_2(\text{dcpm})_2]^{2+}$ .
- Fig. S13** PD total yield dependence on laser repetition rate (327, 490 and 982 Hz).
- Fig. S14** Fragment specific UV-PD yield spectra of  $[\text{Ag}_2(\text{dcpm})_2]^{2+}$ .
- Fig. S15** Comparison between PD and CID mass spectra of species m/z 515 $^{(2+)}$  and m/z 515 $^{(+)}$ .
- Tab. S1** CID fragment assignments for m/z 515 $^{(2+)}$  and m/z 515 $^{(+)}$  precursor species.
- Fig. S16** CID/PD mass spectra of m/z 1065 $^{(+)}$  and m/z 515 $^{(+)}$  (MS $^2$ /MS $^3$  experiments).
- Fig. S17** CID/PD mass spectra of m/z 515 $^{(2+)}$  and m/z 474 $^{(2+)}$ , 433 $^{(2+)}$ , 392 $^{(2+)}$ , 351 $^{(2+)}$ , 310 $^{(2+)}$ , 269 $^{(2+)}$  (Cy)/(Cy -H) loss fragments (MS $^2$ /MS $^3$  experiments).
- Fig. S18** CID/PD mass spectra of m/z 515 $^{(2+)}$  and m/z 462 $^{(2+)}$  (MS $^2$ /MS $^3$  experiments).
- Fig. S19** CID/PD mass spectra of m/z 515 $^{(2+)}$  and m/z 819 $^{(+)}$ , 623 $^{(+)}$  ionic fragment species (MS $^2$ /MS $^3$  experiments).
- Fig. S20** Schematic structure of  $[\text{Ag}_2\text{Hdcpm}]^+$  species (m/z 623).
- Tabs. S2-S4** Comparison between simulated and experimental isotope patterns for  $[\text{Ag}_2(\text{dcpm})_2]^{2+}$  and its fragments.
- Fig. S21** Cross-correlation signals ( $\lambda_{\text{pump}} = 245$  nm, 260 nm, 275 nm;  $\lambda_{\text{probe}} = 1150$  nm) by multiphoton ionization of furan.
- Fig. S22** Transient total fragment yield signals at different mutual polarizations of pump and probe pulses.
- Fig. S23** Decay associated normalized amplitudes of global fit ( $\lambda_{\text{pump}} = 260$  nm,  $\lambda_{\text{probe}} = 1150$  nm).
- Eqs. S1,S2** Fit formula applied to  $\tau$ -PD data.
- Fig. S24** Comparison between tetra- and tri-exponential fit for  $\tau$ -PD total yield of  $[\text{Ag}_2(\text{dcpm})_2]^{2+}$  ( $\lambda_{\text{pump}} = 260$  nm,  $\lambda_{\text{probe}} = 1150$  nm).

**Fig. S25** Tetra-exponential fit for  $\tau$ -PD total yield of  $[\text{Ag}_2(\text{dcpm})_2]^{2+}$  ( $\lambda_{\text{pump}} = 245, 275 \text{ nm}$ ;  $\lambda_{\text{probe}} = 1150 \text{ nm}$ ).

**Fig. S26** Released (global) fit for channel specific  $\tau$ -PD yields of  $[\text{Ag}_2(\text{dcpm})_2]^{2+}$  ( $\lambda_{\text{pump}} = 260 \text{ nm}$ ,  $\lambda_{\text{probe}} = 1150 \text{ nm}$ ).

**Tab. S5** Summary of fit parameters for released (global) fit.

**Tab. S6** Calculated electronic transitions and optimized Ag-Ag distances for  $C_{2h}$ ,  $C_{2v}$  and  $C_2$  conformers of  $[\text{Ag}_2(\text{dmpm})_2]^{2+}$ .

**Fig. S27** Calculated ground state geometries for  $C_{2h}$ ,  $C_{2v}$  and  $C_2$  conformers of  $[\text{Ag}_2(\text{dmpm})_2]^{2+}$ .

**Fig. S28** MO diagram for  $C_{2h}$  and  $C_{2v}$  conformers of  $[\text{Ag}_2(\text{dmpm})_2]^{2+}$ .

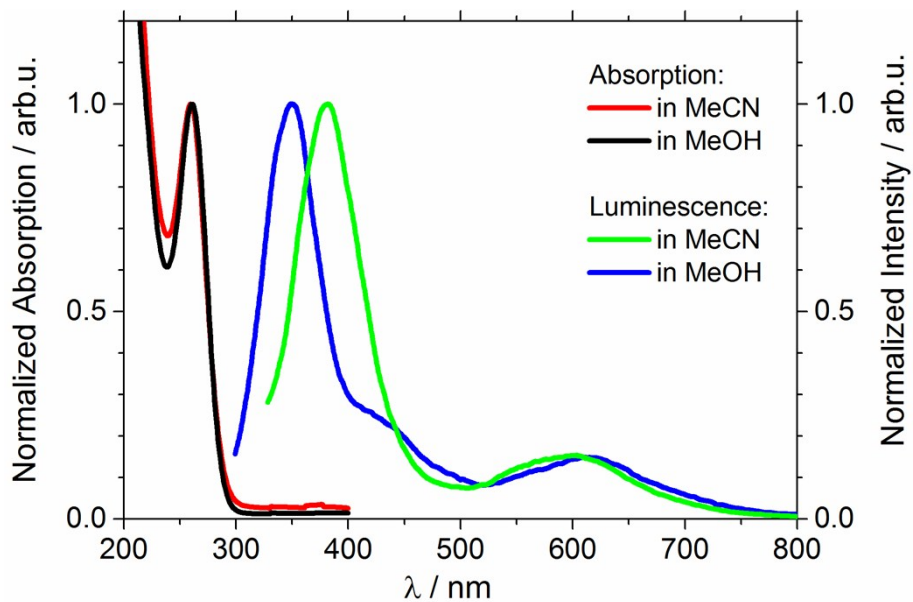
**Fig. S29** Most important NTO pairs for the  ${}^1\text{MC}(\text{d}\sigma^*-\text{p}\sigma)$  transition of  $C_{2h}$  and  $C_{2v}$  conformers of  $[\text{Ag}_2(\text{dmpm})_2]^{2+}$ .

**Tabs. S7-S13** Cartesian coordinates for optimized ground and excited state structures of  $C_{2h}$ ,  $C_{2v}$  and  $C_2$  conformers of  $[\text{Ag}_2(\text{dmpm})_2]^{2+}$ .

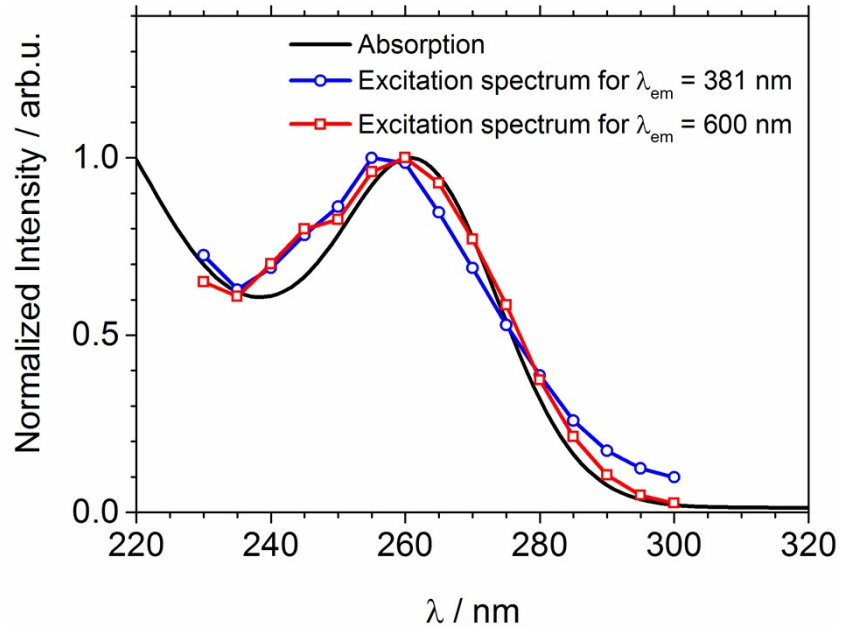
Calculated enthalpies / free enthalpies for Cy/(Cy-H) loss of the  $[\text{Ag}_2\text{L}^{4\text{Me}}\text{L}^{3\text{Me,Cy}}]^{2+}$ ,  $\text{L}^{4\text{Me}} = (\text{Me}_2\text{PCH}_2\text{PMe}_2) = \text{dmpm}$ ,  $\text{L}^{3\text{Me,Cy}} = (\text{Me}_2\text{PCH}_2\text{PMeCy})$  model system.

**Eqs. S3,S5** Homolytic and heterolytic P-C bond dissociation for Cy/(Cy-H) loss.

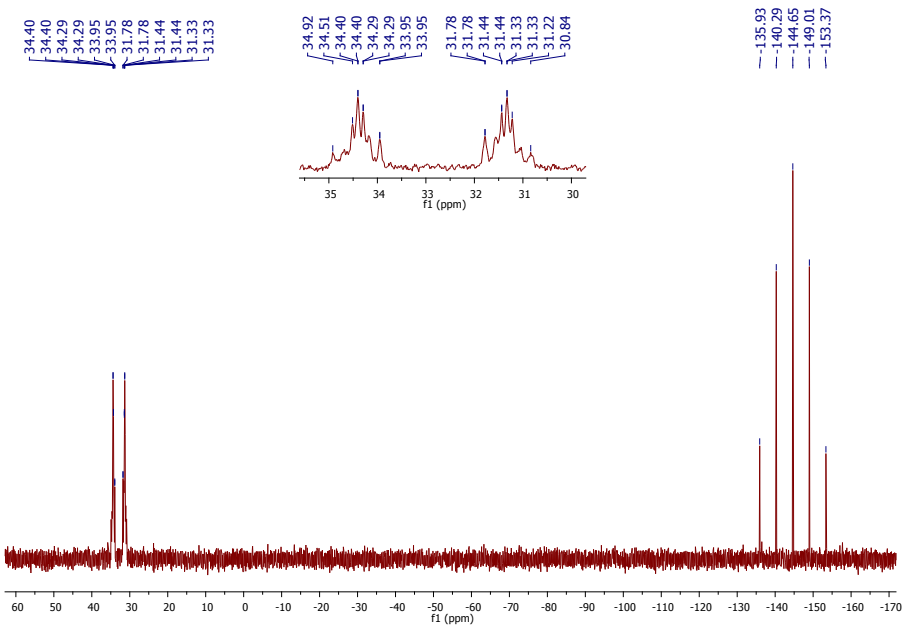
Optimized geometries for the respective  $\text{P}^{2+}$ ,  $\text{F}_1^{2+}$  and  $\text{F}_2^0$  species associated with Eqs. S3-S5 (DFT/B3LYP/cc-pVDZ (H, C, N, O), Stuttgart 1997 ECP (Ag)).



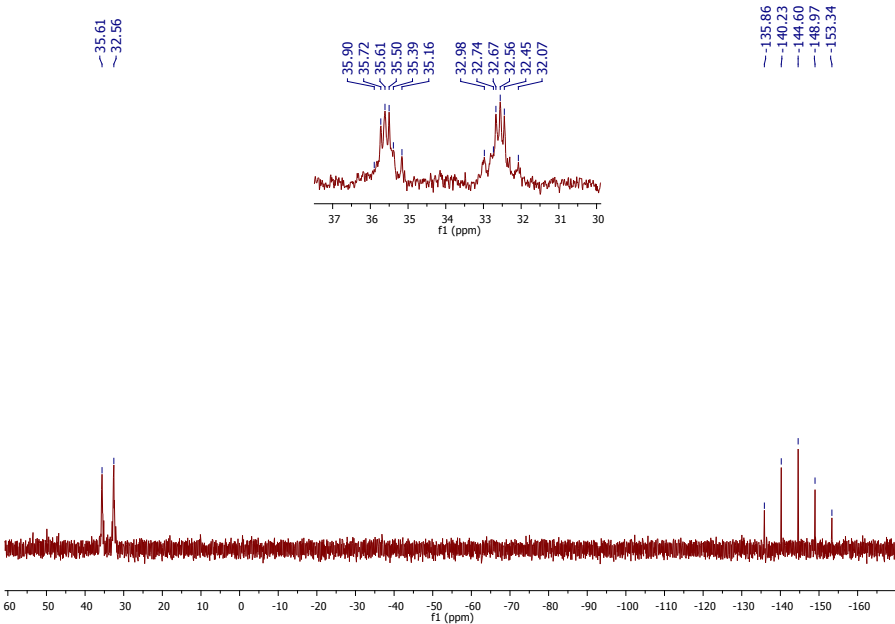
**Fig. S1** Normalized absorption and luminescence spectra of  $[\text{Ag}_2(\text{dcpm})_2](\text{PF}_6)_2$  in MeCN and MeOH, respectively at room temperature (absorption:  $c = 2 \text{ mM}$ , luminescence:  $c = 0.02 \text{ mM}$ ).



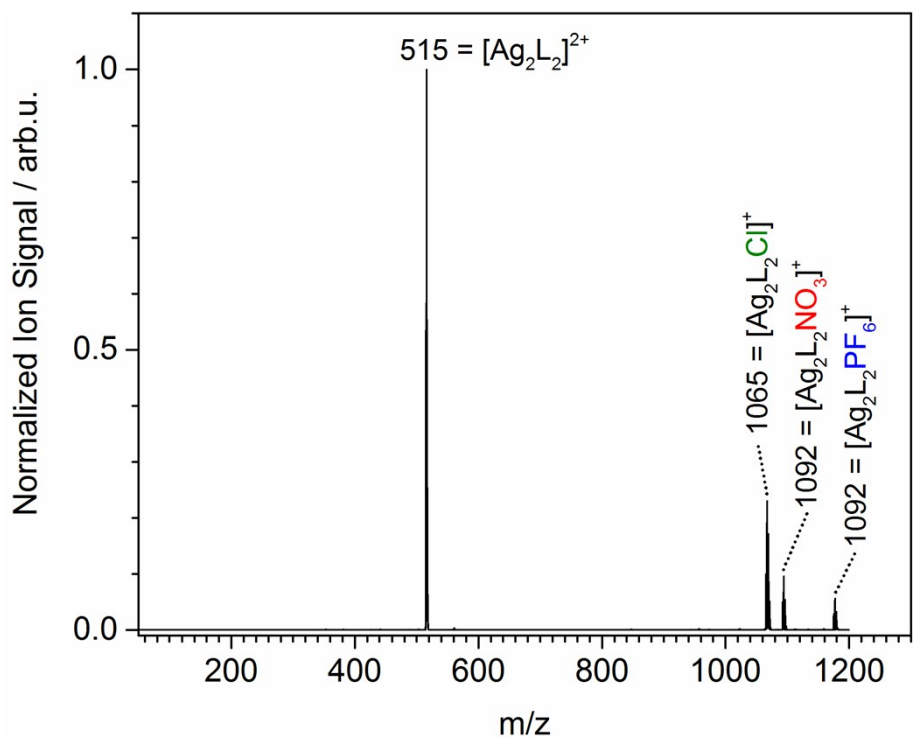
**Fig. S2** Normalized absorption spectrum compared to luminescence excitation spectra for emissions at 381 nm and 600 nm, respectively ( $[\text{Ag}_2(\text{dcpm})_2](\text{PF}_6)_2$  in MeCN, (absorption:  $c = 2 \text{ mM}$ , luminescence:  $c = 0.02 \text{ mM}$ ).



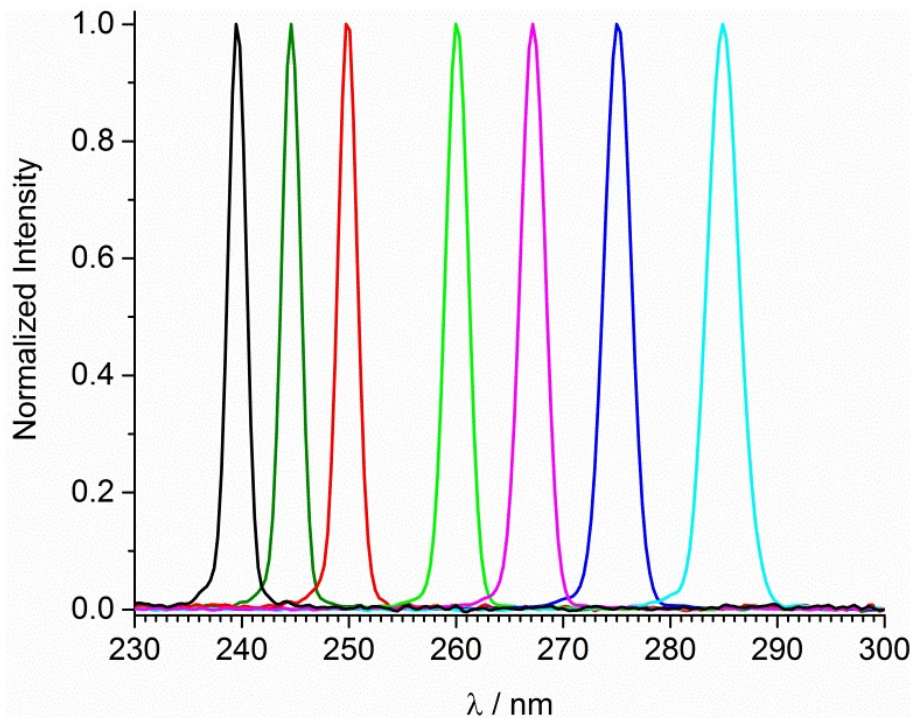
**Fig. S3**  $^{31}\text{P}$ -NMR spectrum of  $[\text{Ag}_2(\text{dcpm})_2](\text{PF}_6)_2$  (168.1 MHz, MeCN-d3):  $\delta/\text{ppm} = 34.92\text{-}30.84$  (dm,  $\text{P}_{\text{dcpm}}$ ), -144.65 (qi,  $\text{P}_{\text{PF}_6}$ ).



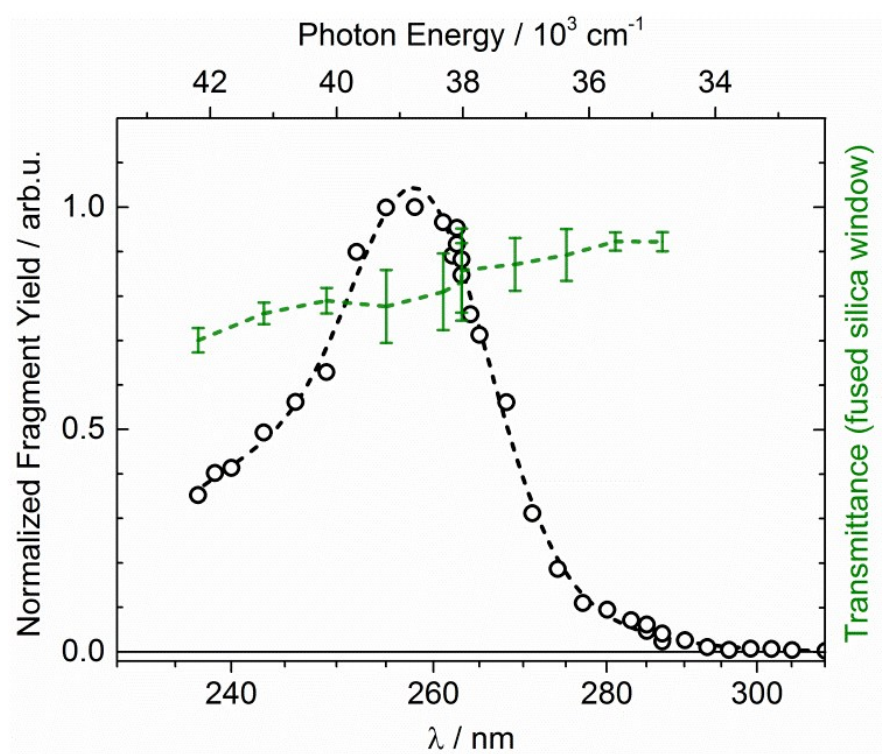
**Fig. S4**  $^{31}\text{P}$ -NMR spectrum of  $[\text{Ag}_2(\text{dcpm})_2](\text{PF}_6)_2$  (168.1 MHz, MeOD-d4):  $\delta$  [ppm] = 35.90-32.07 (dm,  $\text{P}_{\text{dcpm}}$ ), -144.60 (qi,  $\text{P}_{\text{PF}_6}$ ).



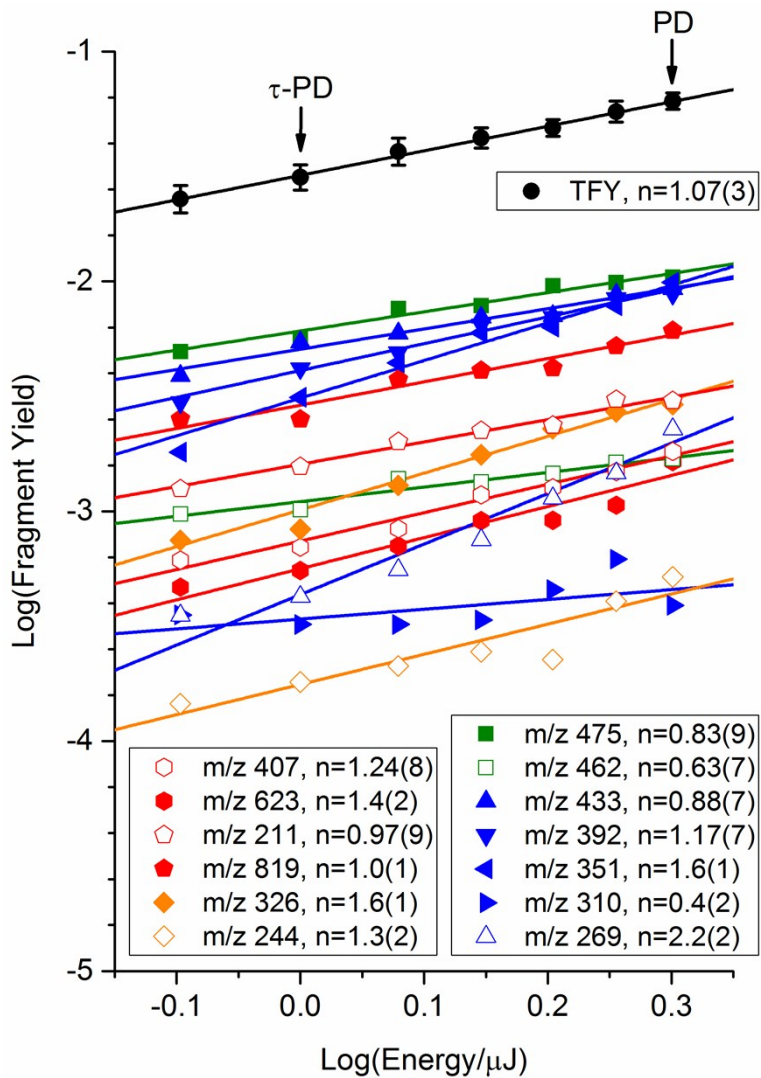
**Fig. S5** Electrospray ionization mass spectrum of a solution of  $[\text{Ag}_2\text{L}_2](\text{PF}_6)_2$  ( $\text{L} = \text{dcpm}$ , bis(dicyclohexylphosphino)methane) dissolved in MeCN ( $c \sim 1\mu\text{M}$ ).



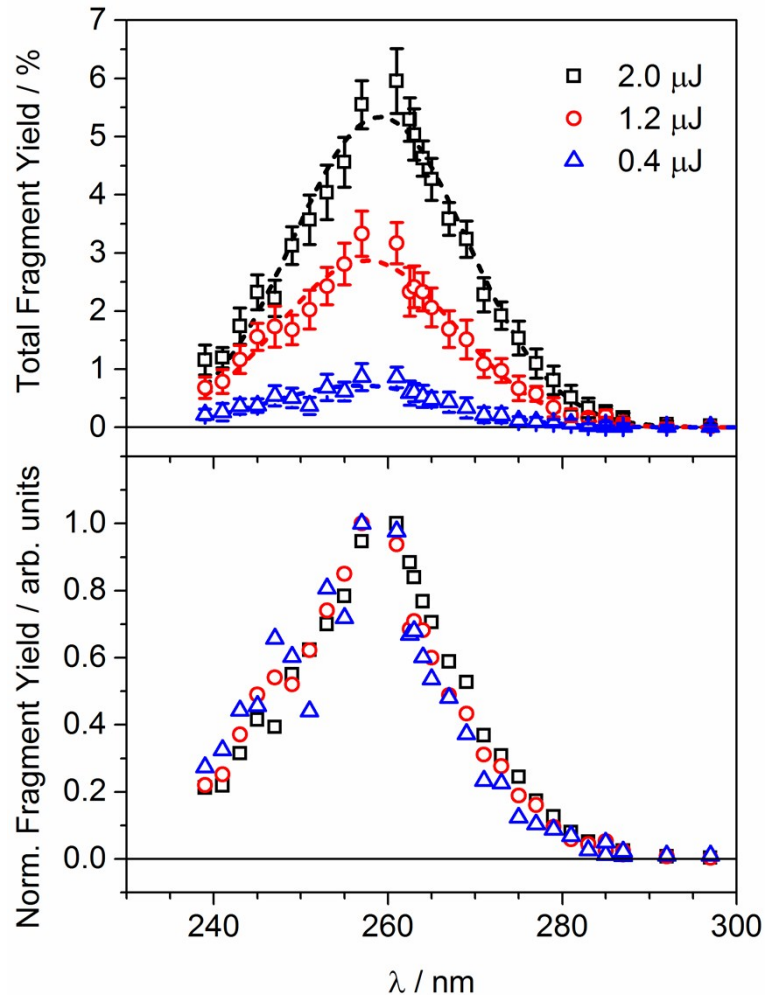
**Fig. S6** Spectral profiles of nonlinear frequency converter output (TOPAS-C, Light Conversion, labeled TC<sub>1</sub>) at various central wavelengths  $\lambda_{\text{central}}/\text{nm}$  (fwhm/nm): 240, 245 (2.1), 250, 260 (2.5), 267.5, 275, 285 (3.5).



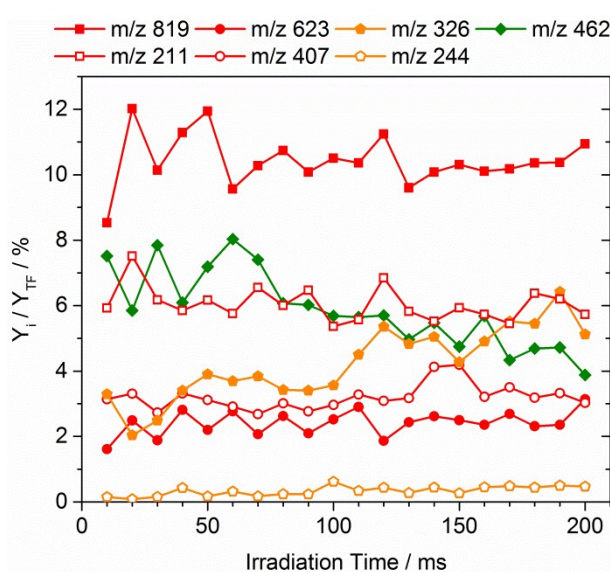
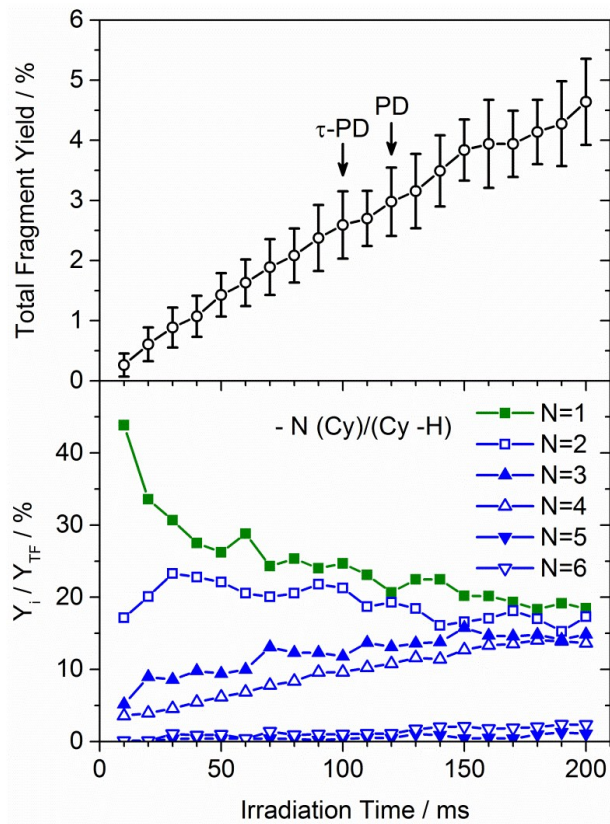
**Fig. S7** UV-PD total yield spectrum of gaseous  $[\text{Ag}_2(\text{dcpm})_2]^{2+}$  ions (open circles, 2  $\mu\text{J}$ , 118 pulses) and transmittance of the fused silica window before the ion trap (green error bars:  $\pm 1\sigma$ ,  $I_{\text{trans.}}/I_0$ , 3 mm thickness) measured outside the trap at approximately equivalent photon density and  $\sim 0^\circ$  angle of incidence.

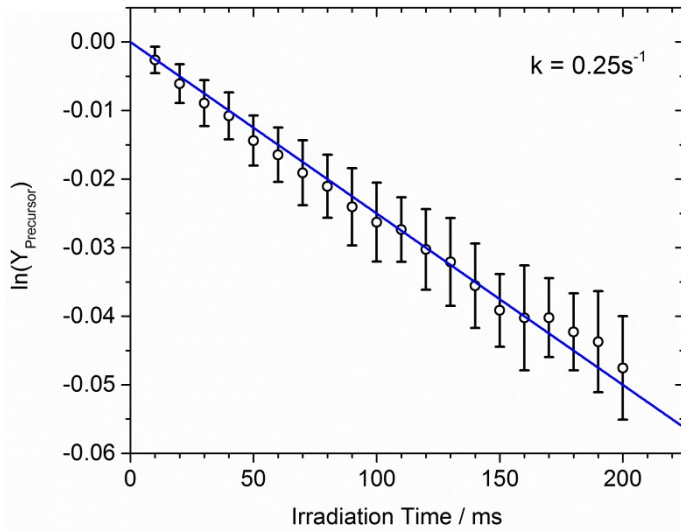


**Fig. S8** Log-log plots for the dependence of fragment specific yields (channels are denoted by nominal masses) on laser intensity ( $\lambda_{\text{ex}} = 263 \text{ nm}$ , range:  $0.8 - 2 \mu\text{J}$ ,  $0.2 \mu\text{J}$  steps). TFY = total fragment yield (error bars:  $\pm 1\sigma$ ). Individual slopes of linear fits are indicated as  $n$  and standard errors are given in parentheses. Laser intensities used for PD and  $\tau$ -PD experiments are highlighted by arrows. Color scheme adapted from Fig. 3.

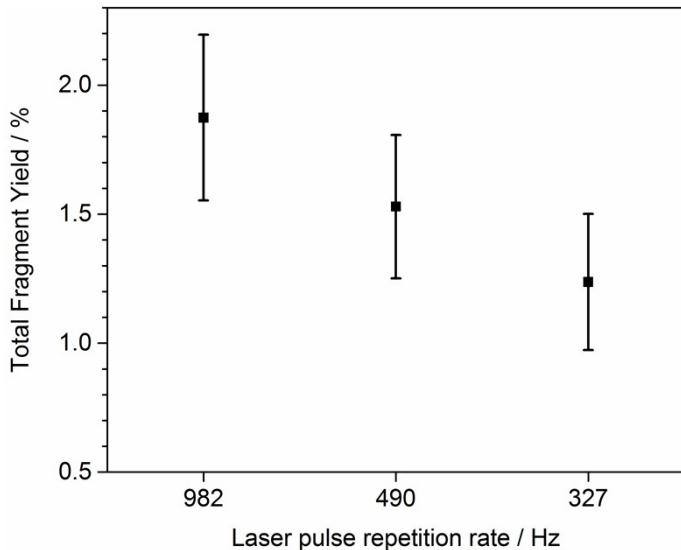


**Fig. S9** (top) Non-normalized UV-PD total yield spectra of gaseous  $[\text{Ag}_2(\text{dcpm})_2]^{2+}$  ions measured at various laser intensities at  $0.4$ ,  $1.2$  and  $2 \mu\text{J}$ , respectively. (bottom) UV-PD total yield spectra normalized to unity in order to compare spectral profiles.

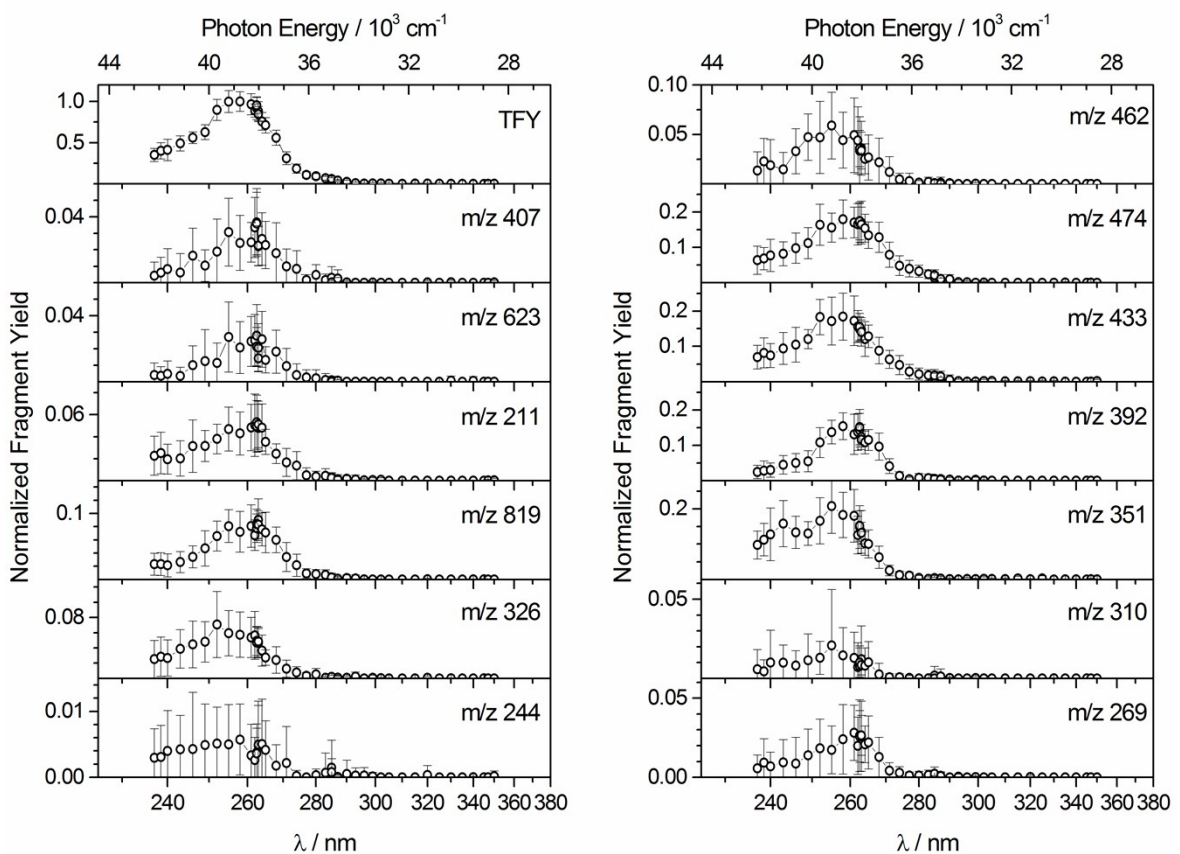




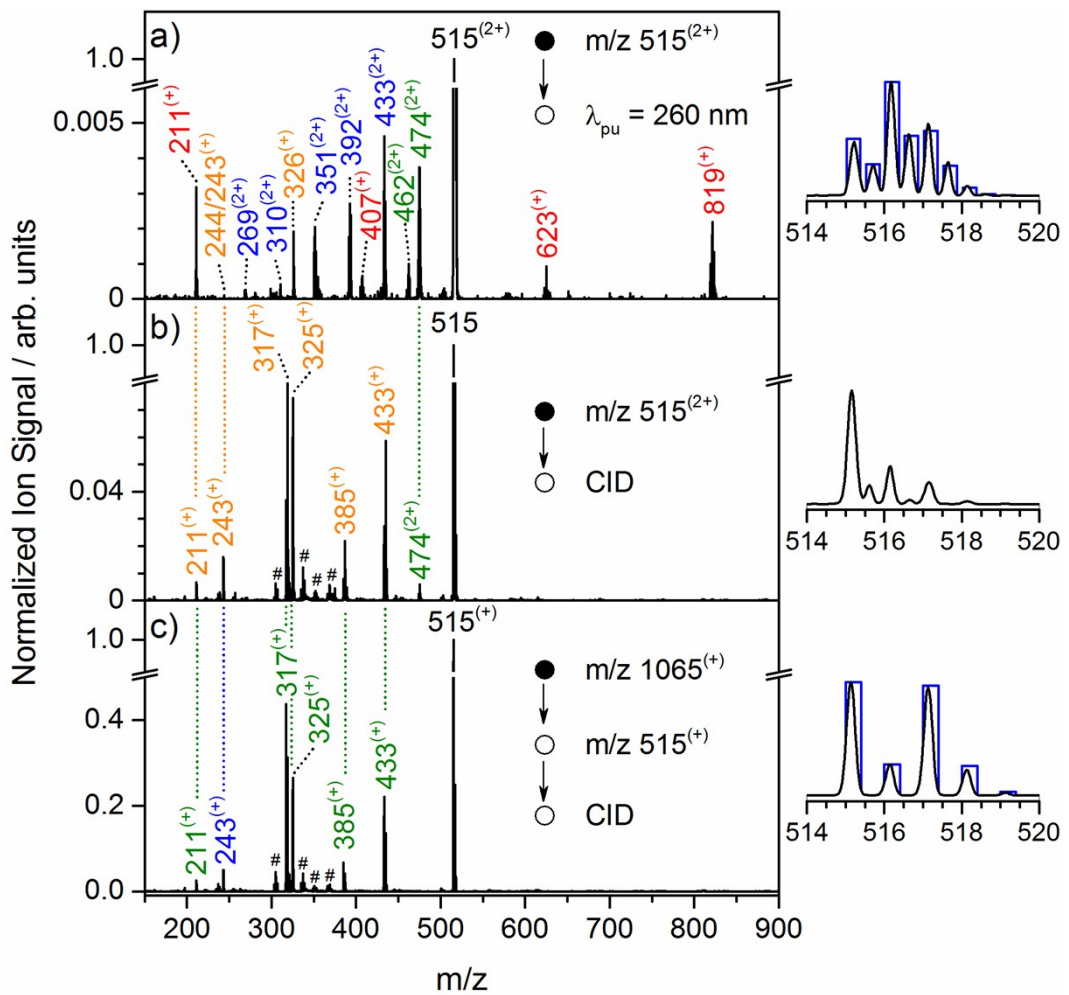
**Fig. S12** Natural logarithm of relative ion abundance of  $[\text{Ag}_2(\text{dcpm})_2]^{2+}$  precursor ( $Y_{\text{Precursor}} = P/(\sum F_i + P)$ , P: precursor ion signal,  $F_i$ : fragment ion signals) as function of irradiation time ( $\lambda_{\text{ex}} = 260$  nm,  $E = 2 \mu\text{J}$ , rep. rate: 982 Hz, error bars:  $\pm 1\sigma$ ). Slope of linear fit (blue line) is denoted as k.



**Fig. S13** UV-PD total fragment yield of  $[\text{Ag}_2(\text{dcpm})_2]^{2+}$  as a function of laser pulse repetition rate (modulated by means of an optical chopper). The number of pulses per isolated ion bunch was kept constant by variation of irradiation time ( $\lambda_{\text{ex}} = 263$  nm,  $E = 2 \mu\text{J}$ , 982 Hz (40 ms), 490 Hz (80 ms), 327 Hz (120 ms)).



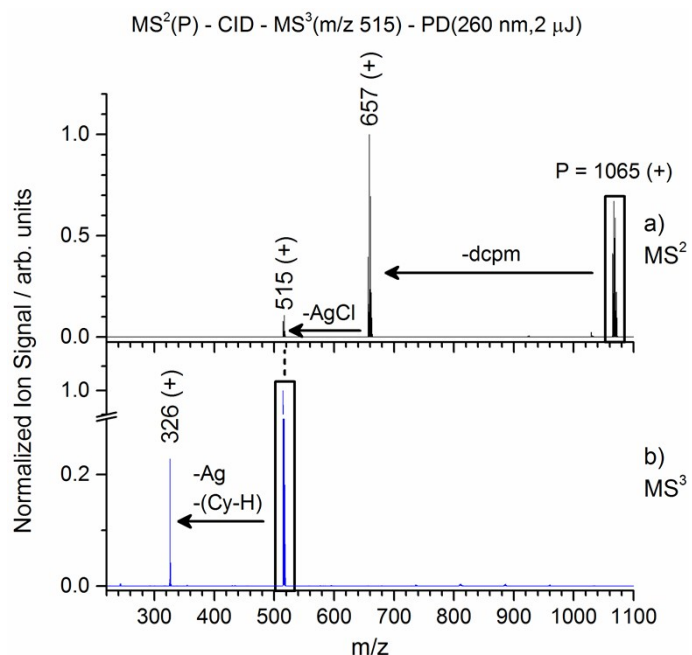
**Fig. S14** Fragment channel specific UV-PD yield spectra (nominal masses are indicated, TFY: total fragment yield,  $E = 2 \mu\text{J}$ , 118 pulses). Spectra are normalized to maximum of the TFY. Error bars represent one standard deviation ( $\pm 1\sigma$ , at least 170 mass spectra).



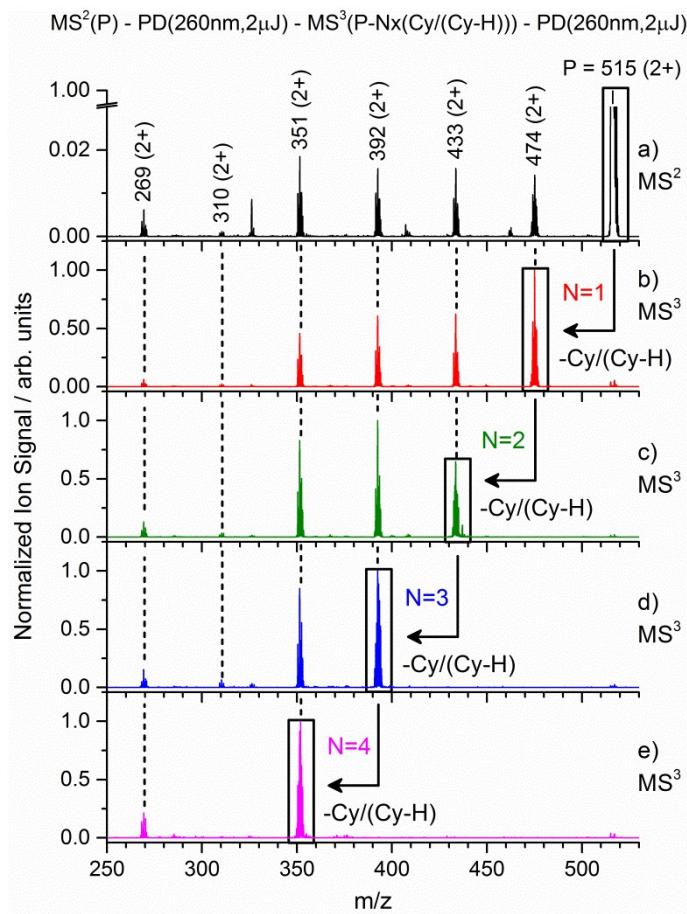
**Fig. S15** a) PD mass spectrum of  $[Ag_2(dcpm)_2]^{2+}$  ( $m/z = 515$ ) at  $\lambda_{ex} = 260$  nm ( $1 \mu J$ ,  $\sim 98$  pulses). Right inset: experimental (black line) and simulated (blue bars) isotope pattern of precursor ions ( $m/z = 515$ ) during irradiation. Nominal masses are indicated (for assignments see Tab. 1) b) CID mass spectrum of  $[Ag_2(dcpm)_2]^{2+}$  ( $m/z = 515$ ) precursor (excitation amplitude = 0.85 V, internal energy scale of mass spectrometer). Right inset: CID mass signal the range of  $m/z = 514-520$  indicating that signals for  $[Ag_2(dcpm)_2]^{2+}$  precursor and  $[Ag(dcpm)]^+$  fragment ions are superimposed. c) CID mass spectrum obtained in MS<sup>3</sup> step corresponding to first CID of isolated  $[Ag_2Cl(dcpm)_2]^+$  precursors ( $m/z = 1065$ , excitation amplitude = 1.3 V), second isolation of  $[Ag(dcpm)]^+$  fragment species ( $m/z = 515$ ) and subsequent collision-induced dissociation (excitation amplitude = 1.2 V). Right inset: experimental (black line) and simulated (blue bars) isotope pattern of isolated  $[Ag(dcpm)]^+$  ions ( $m/z = 515$ ) obtained from  $m/z = 1065$  precursor in MS<sup>3</sup> step without subsequent CID (excitation amplitude = 1.3 V). Pound keys indicate species which could not ambiguously assigned by their isotope pattern. Equal species are connected by colored dotted lines for clarity. Color scheme was adapted from Fig. 3. For fragment assignments for b) and c) see Tab. S1.

**Tab. S1** CID fragment assignments of  $[\text{Ag}_2(\text{dcpm})_2]^{2+}$  precursor ( $m/z$  515) shown in Fig. S15 b). Nominal masses ( $m/z$ ) and charge states ( $z/e$ ) are indicated.  $F_{\text{dark}}$  corresponds to ion signal of  $[\text{Ag}(\text{dcpm})]^+$  fragment which is superimposed with the precursor isotope pattern (see Fig. S15 right inset). For the sake of simplicity the collision-induced fragments are categorized into four groups associated with primary and secondary ionic fragmentation ( $\text{IF}_p$ ,  $\text{IF}_s$ ) and single neutral loss (NL).

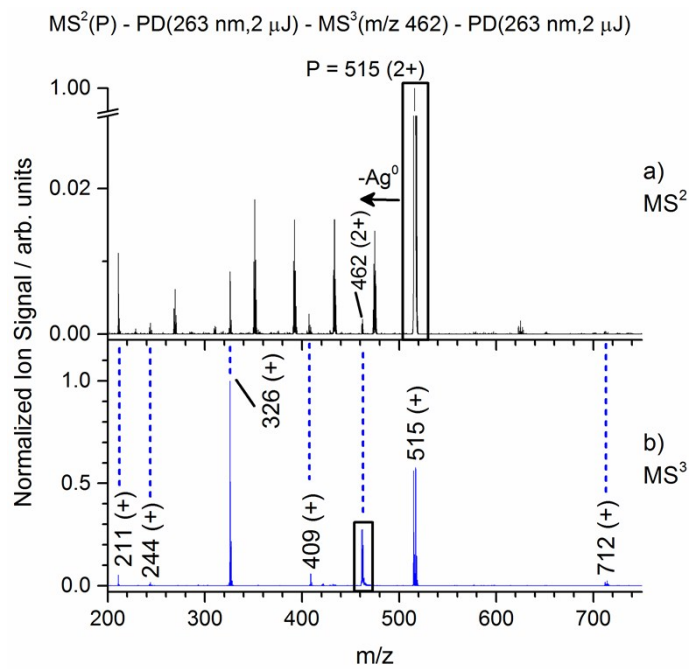
Label	$m/z$	$z/e$	Assigned formula	Fragments lost	Category
P	515	2	$[\text{Ag}_2\text{P}_4(\text{CH}_2)_2(\text{Cy})_8]^{2+}$		Precursor
$F_{\text{dark}}$	515	1	$[\text{AgP}_2(\text{CH}_2)(\text{Cy})_4]^+$	$[\text{AgP}_2(\text{CH}_2)(\text{Cy})_4]^+$	$\text{IF}_p$
$F_1$	474	2	$[\text{Ag}_2\text{P}_4(\text{CH}_2)_2(\text{Cy})_7\text{H}]^{2+}$	(Cy-H)	NL
$F_2$	433	1	$[\text{AgP}_2(\text{CH}_2)(\text{Cy})_3\text{H}]^+$	$[\text{AgP}_2(\text{CH}_2)(\text{Cy})_4]^+$ , (Cy-H)	$\text{IF}_s$
$F_3$	385	1	" $[\text{AgP}(\text{Cy})_3\text{-}2\text{H}]^+$ "	$[\text{AgP}_2(\text{CH}_2)(\text{Cy})_4]^+$ , " $\text{P}(\text{CH}_2)(\text{Cy})\text{+}2\text{H}$ "	$\text{IF}_s$
$F_4$	325	1	$[\text{P}_2(\text{CH}_2)(\text{Cy})_3]^+$	$[\text{AgP}_2(\text{CH}_2)(\text{Cy})_4]^+$ , Ag, (Cy)	$\text{IF}_s$
$F_5$	317	1	$[\text{AgP}(\text{CH})(\text{Cy})_2]^+$	$[\text{AgP}_2(\text{CH}_2)(\text{Cy})_4]^+$ , $\text{P}(\text{Cy})_2\text{H}$	$\text{IF}_s$
$F_6$	243	1	$[\text{P}_2(\text{CH}_2)(\text{Cy})_2\text{H}]^+$	$[\text{AgP}_2(\text{CH}_2)(\text{Cy})_4]^+$ , Ag, (Cy), (Cy-H)	$\text{IF}_s$
$F_7$	211	1	$[\text{P}(\text{CH}_2)(\text{Cy})_2]^+$	$[\text{AgP}_2(\text{CH}_2)(\text{Cy})_4]^+$ , Ag, $\text{P}(\text{Cy})_2$	$\text{IF}_s$



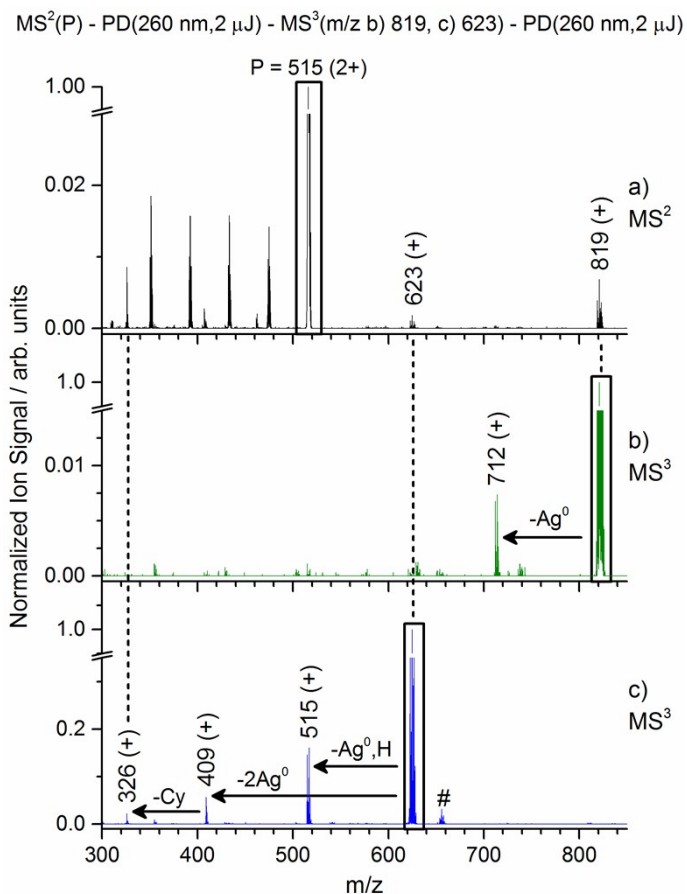
**Fig. S16** a) CID mass spectrum of  $[\text{Ag}_2\text{Cl}(\text{dcpm})_2]^+$  ( $m/z$  1065,  $\text{MS}^2$ ,  $\text{Amp}_{\text{ex}} = 1\text{V}$ ) and b) isolation of  $[\text{Ag}(\text{dcpm})]^+$  ( $m/z$  515) in  $\text{MS}^3$  step with subsequent photodissociation (260 nm, 2  $\mu\text{J}$ ,  $\sim 118$  pulses). Spectra are normalized to most abundant species. Nominal masses and losses are indicated. Charge states ( $z/e$ ) are given in parentheses.



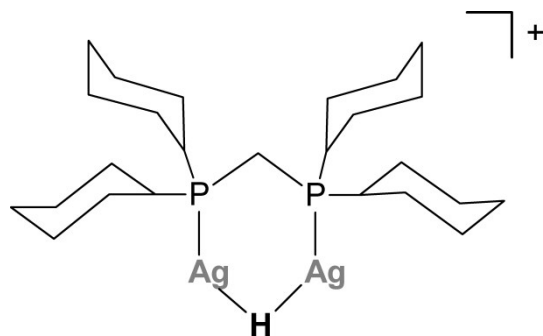
**Fig. S17** a) PD mass spectrum of  $[\text{Ag}_2(\text{dcpm})_2]^{2+}$  ( $m/z$  515) at  $\lambda_{\text{ex}} = 260$  nm ( $2 \mu\text{J}$ ,  $\sim 118$  pulses, MS<sup>2</sup> step) and isolation of photofragments corresponding to  $\text{N}(\text{ Cy}) + (\text{Cy -H})$  losses ( $\text{N}= 1-4$ , b)-e) ) with subsequent photo-induced dissociation (260 nm,  $2 \mu\text{J}$ ,  $\sim 118$  pulses) in a MS<sup>3</sup> step. Fragment assignments are given in Tab. 1. Nominal masses and losses are indicated. Charge states (z/e) are given in parentheses.



**Fig. S18** a) PD mass spectrum of  $[\text{Ag}_2(\text{dcpm})_2]^{2+}$  ( $\text{m/z } 515$ ,  $\lambda_{\text{ex}} = 263 \text{ nm}$ ,  $2 \mu\text{J}$ ,  $\sim 118$  pulses,  $\text{MS}^2$  step) and b) isolation of photofragment corresponding to  $\text{Ag}^0$  loss ( $\text{m/z } 462$ ) with subsequent PD (same conditions used in a),  $\text{MS}^3$  step). Fragment assignments are given in Tab. 1. Nominal masses and losses are indicated. Charge states (z/e) are given in parentheses.

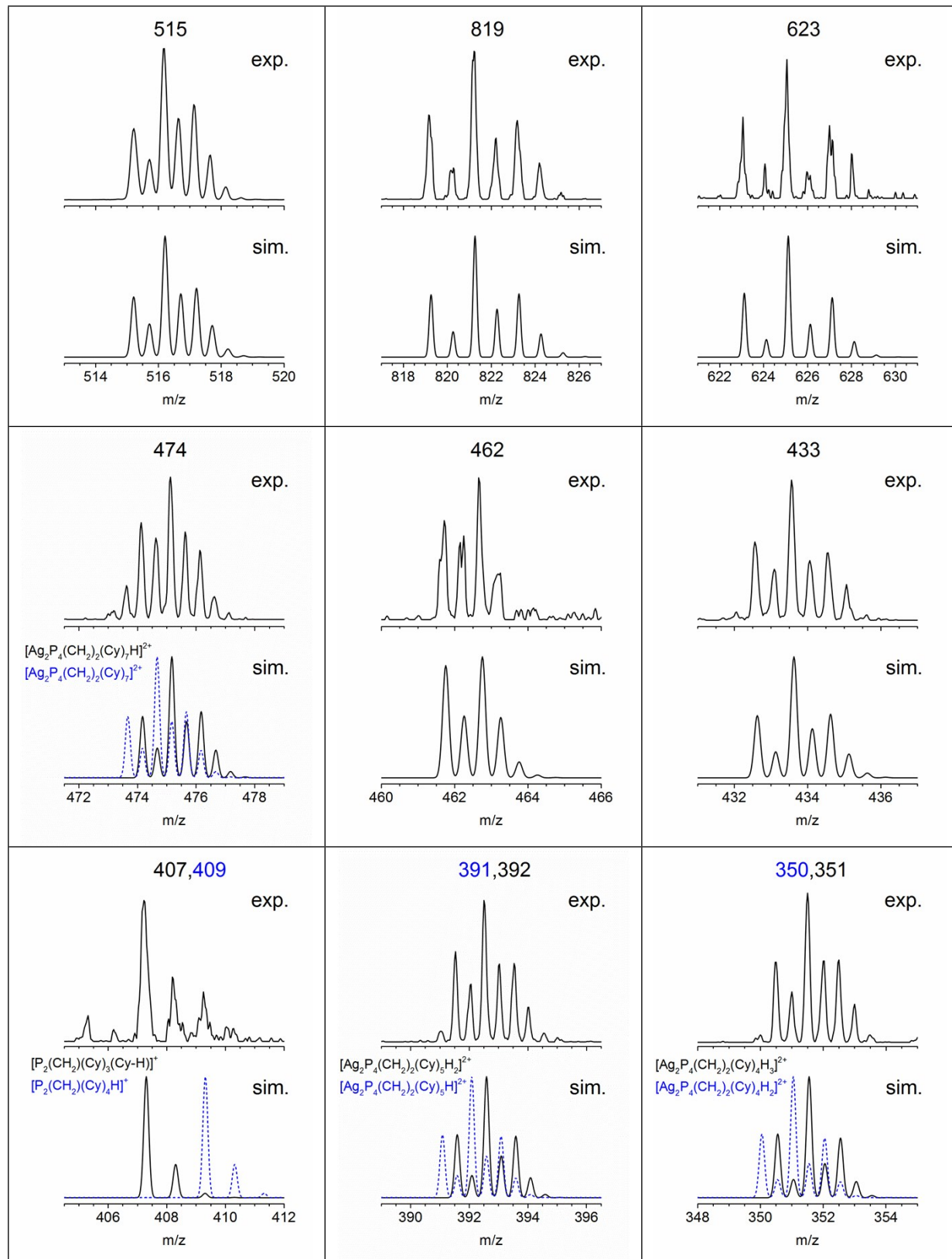


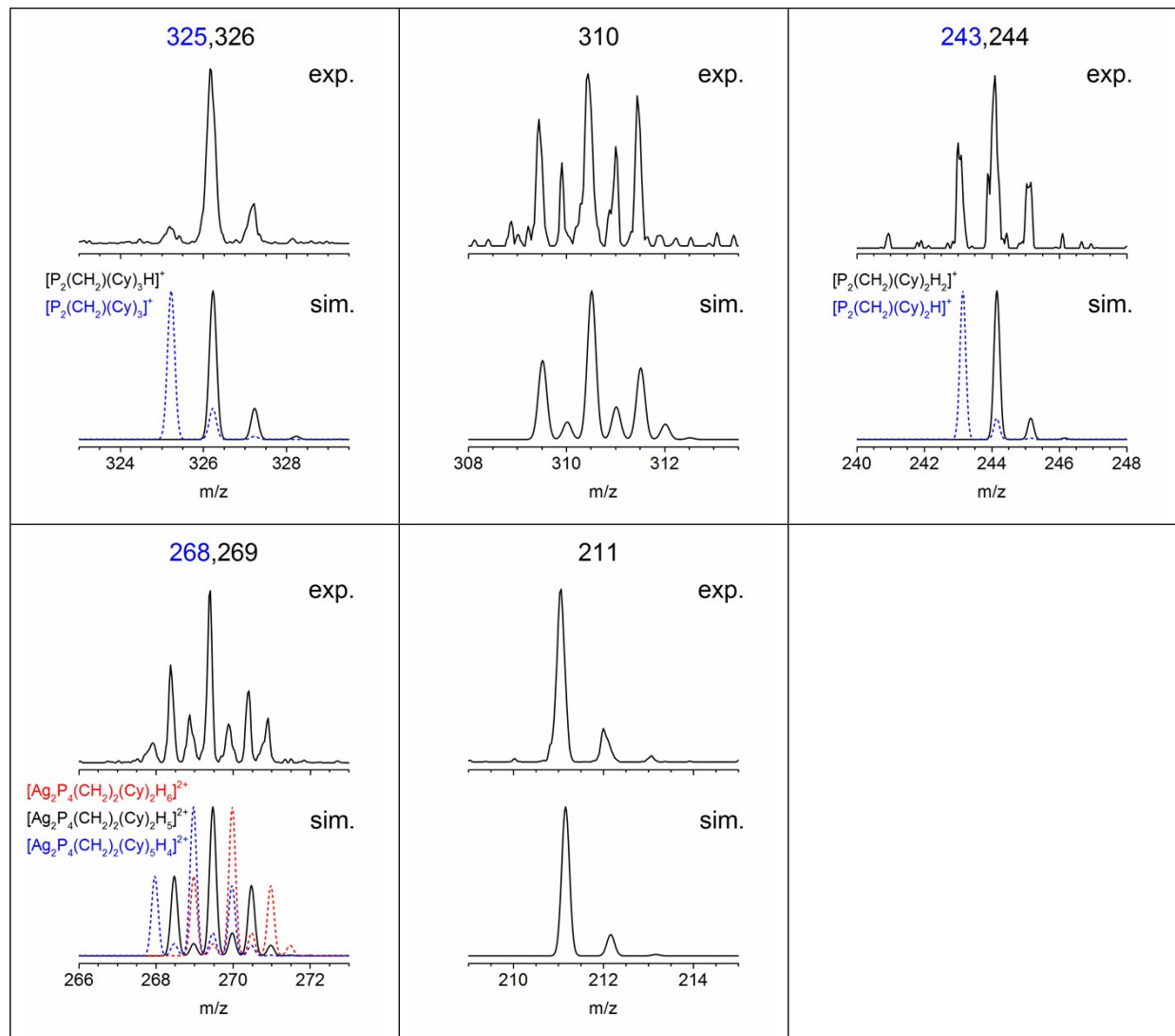
**Fig. S19** a) PD mass spectrum of  $[\text{Ag}_2(\text{dcpm})_2]^{2+}$  ( $m/z$  515,  $\lambda_{\text{ex}} = 260$  nm, 2  $\mu$ J, ~ 118 pulses,  $\text{MS}^2$  step) and isolation of photofragments a)  $m/z$  819 and b)  $m/z$  623, respectively with subsequent PD (same conditions used in a),  $\text{MS}^3$  step). Fragment assignments are given in Tab. 1. Nominal masses and losses are indicated. Charge states (z/e) are given in parentheses. Pound key indicate a gas phase reaction product of  $m/z$  623 species (+ 31 amu) which was not unambiguously assigned.



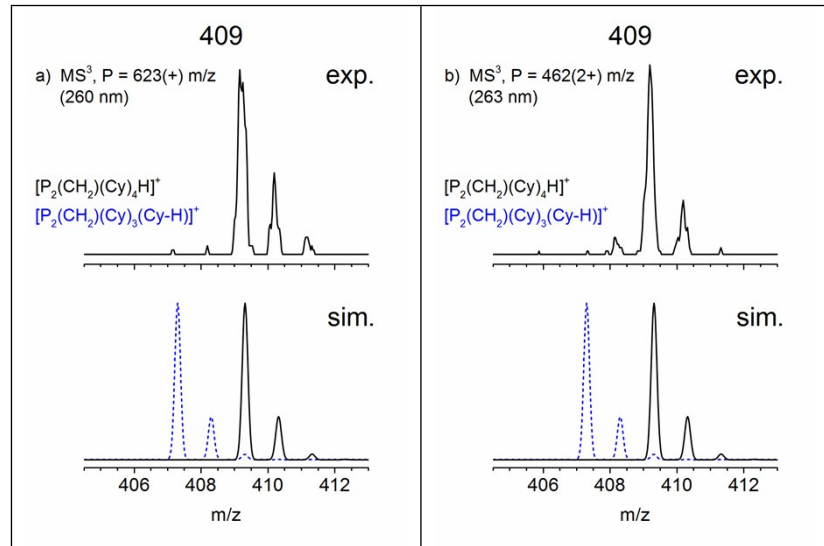
**Fig. S20** Schematic structure of  $[\text{Ag}_2\text{Hdcpm}]^+$  species ( $m/z$  623). A similar species was observed in refs. [1-4]

**Tab. S2** Simulated (Gaussian, fwhm = 0.2) and experimental isotope patterns of  $[\text{Ag}_2(\text{dcpm})_2]^{2+}$  precursor ( $m/z$  515) and its photofragments ( $\lambda_{\text{ex}} = 263$  nm,  $E = 2\mu\text{J}$ , ~118 pulses). Fragment assignments are given in Tab. 1. Nominal masses are indicated. The mass ( $m/z$ ) discrepancy of ~0.1 between experiment and simulation is due to calibration of the MS. Simulations were generated using the Compass Data Analysis software package (Bruker).

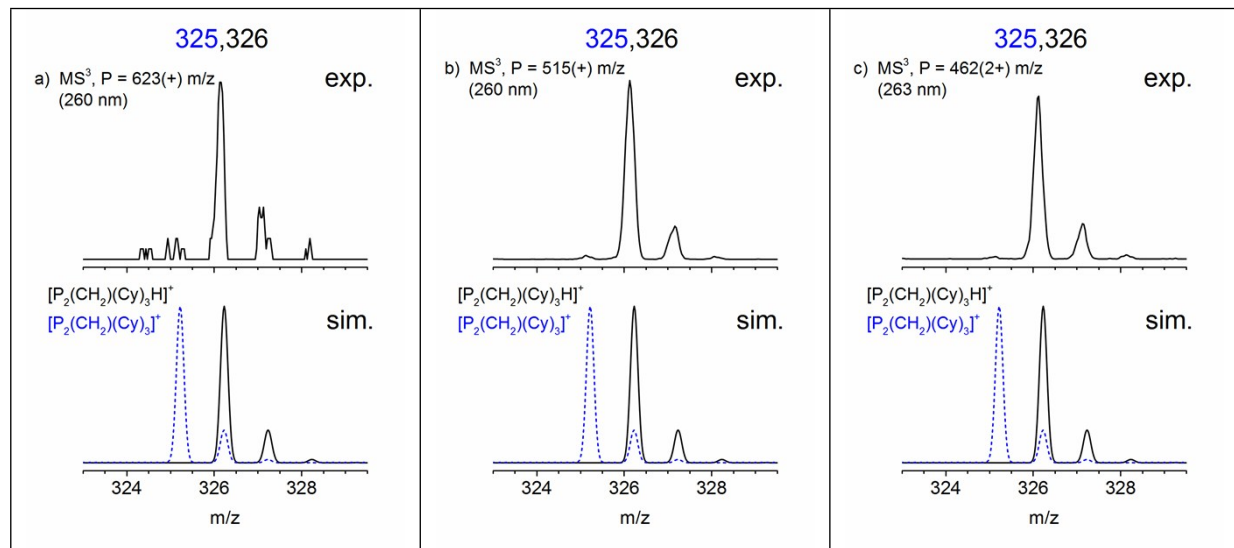




**Tab. S3** Simulated (Gaussian, fwhm = 0.2) and experimental isotope patterns of photofragment m/z 409 obtained from PD of a) m/z 623 (260 nm, 2  $\mu$ J, ~ 118 pulses) and b) m/z 462 precursors (263 nm, 2  $\mu$ J, ~ 118 pulses) in a MS<sup>3</sup> step as shown in Fig. S19 c) and Fig. S18 b), respectively. Nominal masses are indicated.



**Tab. S4** Simulated (Gaussian, fwhm = 0.2) and experimental isotope patterns of photofragment m/z 325/326 obtained from PD of a) m/z 623 (260 nm, 2  $\mu$ J, ~ 118 pulses), b) m/z 515 (monokation, 260 nm, 2  $\mu$ J, ~ 118 pulses ) and c) m/z 462 (263 nm, 2  $\mu$ J, ~ 118 pulses) in a MS<sup>3</sup> step as shown in Figs S19 c), S16 b) and S18 b). Nominal masses are indicated.



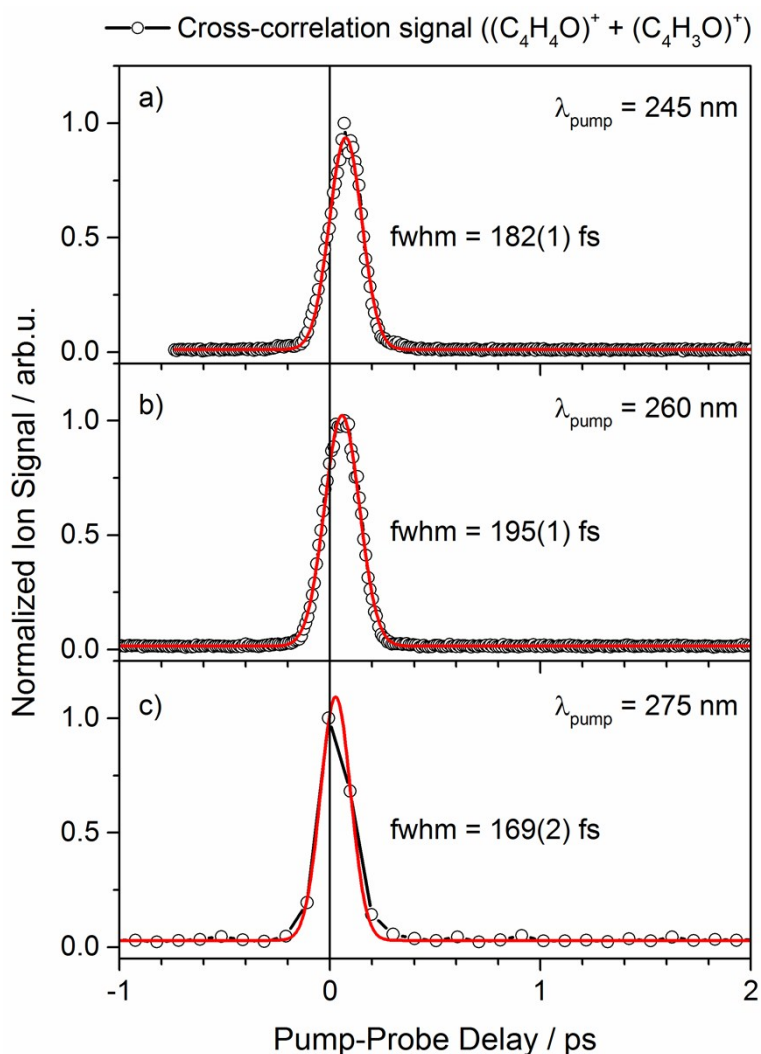


**Fig. S21** Cross-correlation signals as a function of time delay between UV-pump ( $\lambda_{\text{pump}} = \text{a}) 245 \text{ nm}$ , b)  $260 \text{ nm}$ , c)  $275 \text{ nm}$ ;  $1 \mu\text{J}$ ;  $\sim 98$  pulses ) and NIR-probe pulses ( $\lambda_{\text{probe}} = 1150 \text{ nm}$ ; a)  $150 \mu\text{J}$ , b)  $160 \mu\text{J}$ , c)  $150 \mu\text{J}$ ;  $\sim 98$  pulses) measured by multiphoton ionization of neutral furan molecules introduced into the ion trap (sum of integrated ion signals corresponding to  $(\text{furan})^+$  and  $(\text{furan} - \text{H})^+$ , respectively). The time zero position was extracted from kinetic fits of transient PD total yield signals of  $[\text{Ag}_2(\text{dcpm})_2]^{2+}$  measured in parallel (see Tab. 3, Fig. 7). The width (fwhm) of Gaussian fits and standard errors (in parentheses) are indicated.

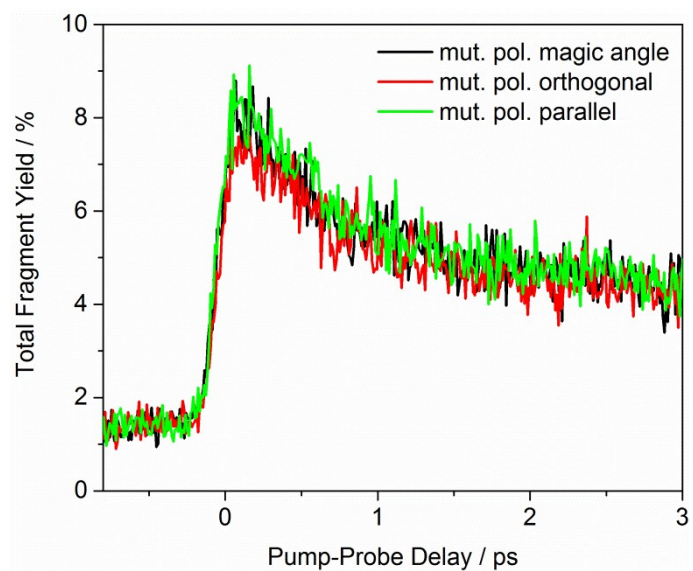


**Fig. S22** Transient total fragment yield of  $[\text{Ag}_2(\text{dcpm})_2]^{2+}$  at  $\lambda_{\text{pump}} = 260 \text{ nm}$  ( $1 \mu\text{J}$ ) and  $\lambda_{\text{probe}} = 1150 \text{ nm}$  ( $145 \mu\text{J}$ ) measured at different mutual polarizations of pump and probe pulses.

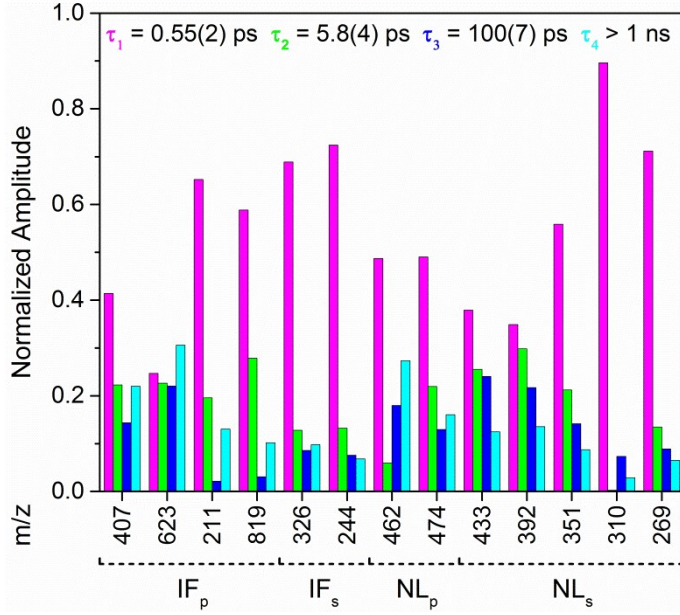


**Fig. S23** Decay associated normalized amplitudes of global fit shown in Fig. 6 ( $\lambda_{\text{pump}} = 260 \text{ nm}$ ,  $\lambda_{\text{probe}} = 1150 \text{ nm}$ ) as a function of channels-specific transients ( $nA_i = A_i / (\sum_i A_i) \times 100$ , colored column bars related to time constants  $\tau_1$ (purple),  $\tau_2$ (green),  $\tau_3$ (blue) and  $\tau_4$ (cyan), respectively). The parameters obtained from fit of the total fragment yield signal (see Tab. 3) was used only releasing the respective ordinate offsets and decay associated amplitudes for global channel-specific fit. Channels are indicated by nominal masses and categorized into primary, secondary ionic fragments ( $\text{IF}_p$ ,  $\text{IF}_s$ ), and single, multiple neutral loss ( $\text{NL}_p$ ,  $\text{NL}_s$ ) fragmentation processes.

#### Formula used for fitting $\tau$ -PD data:

$$F(t) = F_0 + \sum_{i=1}^n A_i \cdot 0.5 \cdot \exp \left( 0.5 \left( \frac{w}{\tau_i} \right)^2 - \frac{(t-t_0)}{\tau_i} \right) \cdot \left( 1 + \operatorname{erf} \left( \frac{1}{\sqrt{2}} \left( \frac{(t-t_0)}{w} - \frac{w}{\tau_i} \right) \right) \right) \quad (\text{Eq. S1})$$

$F_0$ : y-offset, n: number of time constants  $\tau_i$ ,  $A_i$ : decay associated amplitudes,  $w$ : width of Gaussian,  $t_0$ : time zero,  $\exp()$ :exponential function,  $\operatorname{erf}()$ : error function. Relationship between width of Gaussian  $w$  and  $fwhm$  (full width at half maximum) is given by formula (Eq. S2).

$$fwhm = 2\sqrt{2 \ln(2)} \cdot w \quad (\text{Eq. S2})$$

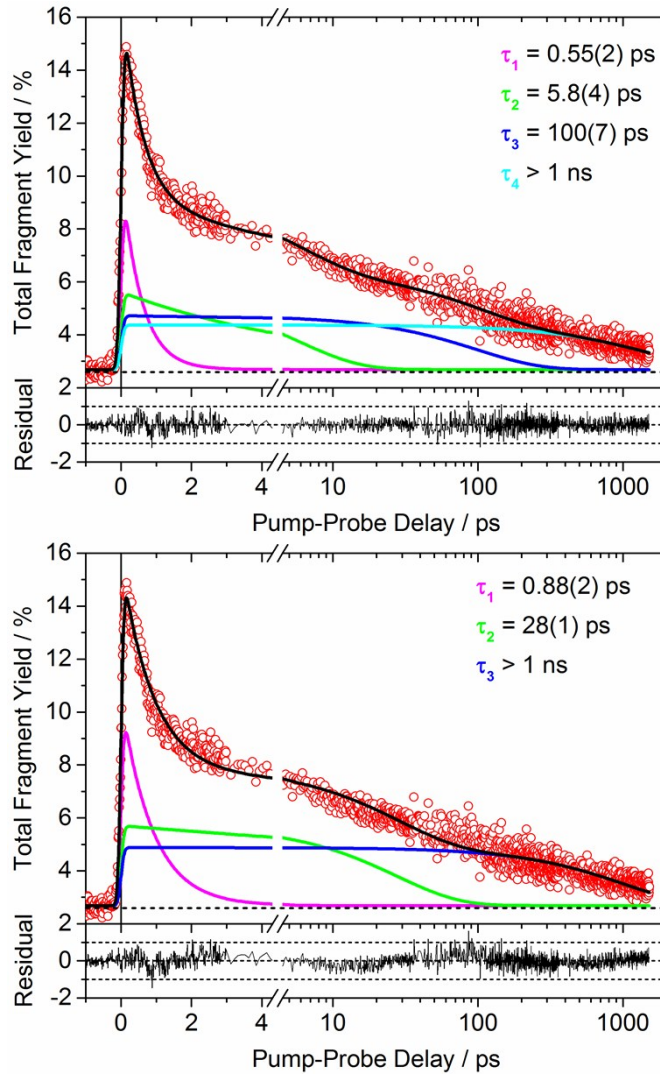


**Fig. S24** Transient PD total yield signal (open circles) of  $[\text{Ag}_2(\text{dcpm})_2]^{2+}$  ( $\lambda_{\text{pump}} = 260$  nm, 1  $\mu\text{J}$ ;  $\lambda_{\text{probe}} = 1150$  nm, 160  $\mu\text{J}$ ) and best kinetic fits (parallel model) by convolution a Gaussian function (top: fwhm = 185(5) fs, bottom: fwhm = 170(5) fs) with a **tetra**-exponential (top, see Fig. 7 b)) and **tri**-exponential (bottom) decay function, respectively. Time delay after 4.5 ps is plotted on a logarithmic scale. Time constants, standard errors (in parentheses) and their individual relaxation contributions (colored solid lines,  $\tau_1$ : magenta,  $\tau_2$ : green,  $\tau_3$ : blue,  $\tau_4$ : cyan) are shown. The pump-only fragmentation yield is indicated as dashed line (negligible probe-only PD yield). Residual plots are shown in the respective lower panels.

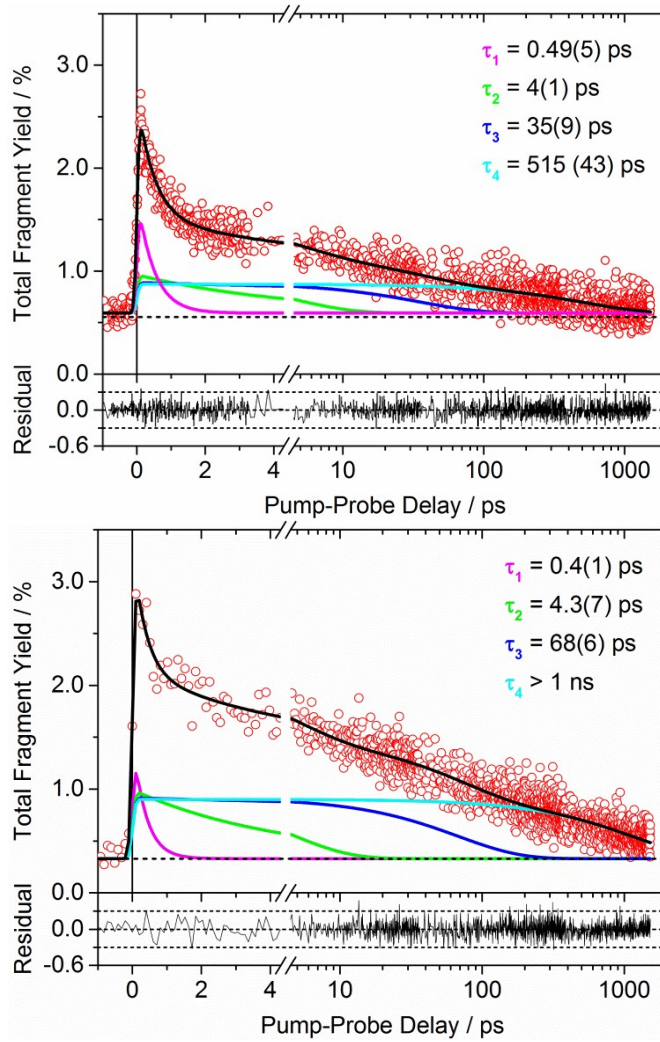


**Fig. S25** Transient PD total yield signals (open circles) of  $[\text{Ag}_2(\text{dcpm})_2]^{2+}$  at different pump excitation wavelengths at  $\lambda_{\text{pump}} = 245 \text{ nm}$  (top) and  $\lambda_{\text{pump}} = 275 \text{ nm}$  (bottom) and kinetic fits shown in Fig. 7 a) and c), respectively ( $\lambda_{\text{probe}} = 1150 \text{ nm}$ , see Tab. 3). Time constants, standard errors (in parentheses) and their individual relaxation contributions (colored solid lines,  $\tau_1$ : magenta,  $\tau_2$ : green,  $\tau_3$ : blue,  $\tau_4$ : cyan) are shown. The pump-only fragmentation yield is indicated as dashed line (negligible probe-only PD yield). Residual plots are shown in the respective lower panels.

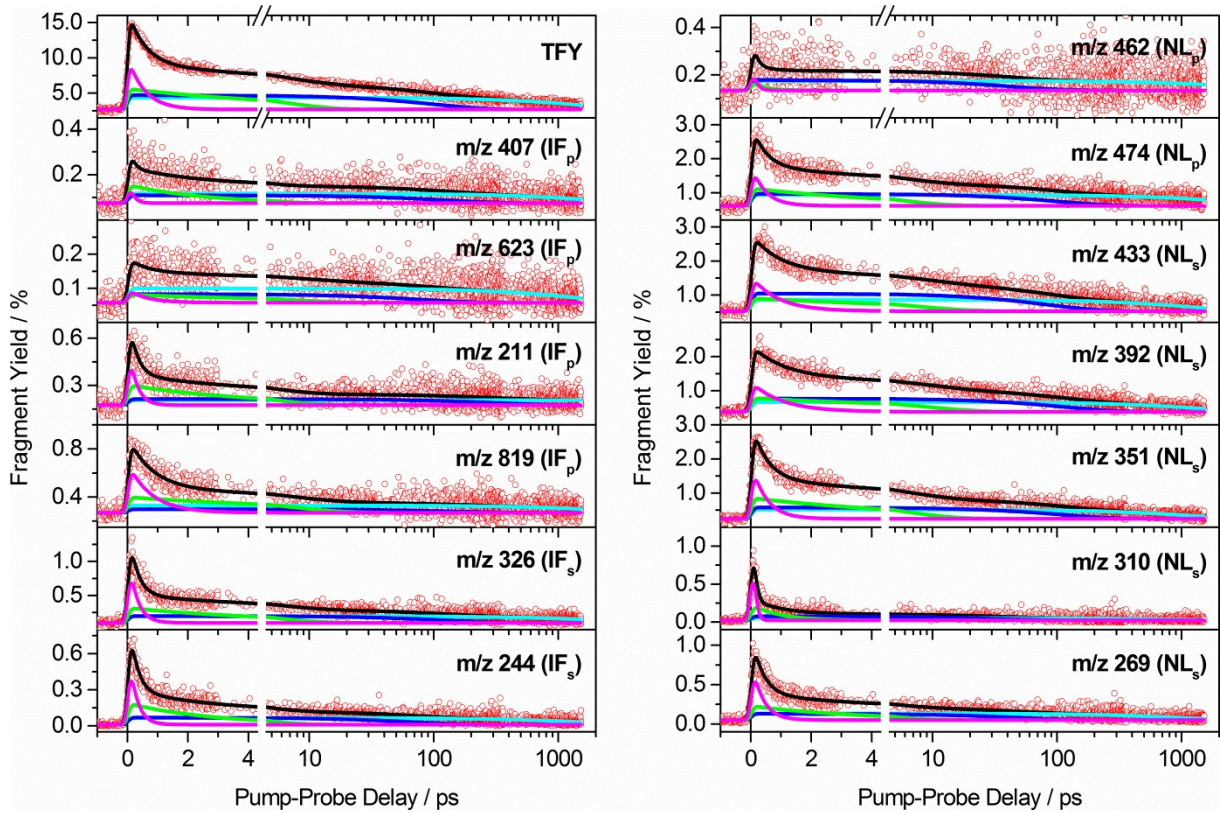


**Fig. S26** Comparison between the  $\tau$ -PD total fragmentation yield signal (TFY) and its individual channel-specific transients of  $[\text{Ag}_2(\text{dcpm})_2]^{2+}$  ( $\lambda_{\text{pump}} = 260 \text{ nm}$ ,  $\lambda_{\text{probe}} = 1150 \text{ nm}$ ). Fragment specific yield signals were globally fitted (black lines) with  $t_0$  and  $w$  as global parameters (see Eq. SF1) releasing all other parameters as summarized in Tab. S4. Individual relaxation contributions are shown as colored lines ( $\tau_1$ : magenta,  $\tau_2$ : green,  $\tau_3$ : blue,  $\tau_4$ : cyan), time delay after 4.5 ps is plotted on a logarithmic scale.

**Tab. S5** Summarized parameters for global fit shown in Fig. S26. IRF: fwhm = 212(3) fs. Errors given in parentheses correspond to standard errors.

Frag. channel	$\tau_1/\text{ps}$	$\tau_2/\text{ps}$	$\tau_3/\text{ps}$	$\tau_4/\text{ps}$
TFY	0.55(2)	5.8(4)	100(7)	1564(94)
m/z 407	0.14(17)	2.4(1.2)	129(116)	1700(1236)
m/z 623	0.64(1.11)	6.8(17.8)	78(129)	1334(809)
m/z 211	0.25(5)	4.0(1.3)	320(151)	$\infty$
m/z 819	0.78(13)	7.1(2.9)	148(-)	2340(-)
m/z 326	0.27(2)	4.7(1.0)	125(45)	2384(1088)
m/z 244	0.25(4)	2.7(9)	66(35)	1522(606)
m/z 462	0.12(43)	0.4(1.9)	42(20)	3033(1924)
m/z 474	0.45(3)	4.8(5)	100(9)	2576(278)
m/z 433	0.88(6)	7.5(1.4)	83(7)	1171(86)
m/z 392	1.04(9)	8.8(1.5)	115(14)	1343(150)
m/z 351	0.49(2)	5.6(5)	109(13)	1135(123)
m/z 310	0.07(1)	0.9(3)	33(17)	984(586)
m/z 269	0.36(4)	3.4(1.3)	50(23)	942(230)
average	0.44(17)	4.5(2.5)	108(45)	1574(547)

**Tab. S6** Calculated (CC2/def2-TZVPP) electronic adiabatic transitions, absorptions (vertical), emissions (vertical) and optimized Ag-Ag distances for  $C_{2h}$ ,  $C_{2v}$  and  $C_2$  conformers of the  $[\text{Ag}_2(\text{dmpm})_2]^{2+}$  (dmpm= bis(dimethylphosphino)methane) model complex, respectively.

Theory						
Species (Level of Theory)	Point group	State (Sym.)	Adiab. trans. / eV	Vert. trans. / eV, $\lambda_{\text{abs}} / \text{nm}$ (oscillator strength)	Vert. em. / eV, $\lambda_{\text{em}} / \text{nm}$ (oscillator strength)	d(Ag-Ag) / Å
$[\text{Ag}_2(\text{dmpm})_2]^{2+}$ (CC2/TZVPP)	$C_{2h}$	$S_0 (^1A_g)$				2.94
		$S_1 (^1B_g)$	4.15	4.48, 277	3.88, 319	2.58
		$S_2 (^1A_u)$	4.43	4.64, 267 (0.41)	4.25, 292 (0.38)	2.66
		$T_1 (^3A_u)$	3.89	4.09, 303	3.74, 332	2.66
		$T_2 (^3B_g)$	3.89	4.16, 298	3.66, 339	2.61
	$C_{2v}$	$S_0 (^1A_1)$				2.94
		$S_1 (^1B_1)$	4.11	4.47, 277 (0.013)	3.77, 328 (0.018)	2.58
		$S_2 (^1B_1)$	n.a.	4.65, 267 (0.39)	n.a.	n.a.
		$T_1 (^3B_1)$	n.a.	4.08, 304	n.a.	n.a.
		$T_2 (^3B_1)$	3.84	4.17, 297	3.54, 350	2.61
	$C_2$	$S_0 (^1A)$				2.91
		$S_1 (^1B)$	4.13	4.48, 277 (0.004)	3.82, 324 (0.008)	2.56
		$S_2 (^1A)$	4.45	4.67, 266 (0.41)	4.25, 292 (0.38)	2.66
		$T_1 (^3A)$	3.90	4.10, 302	3.74, 331	2.66
		$T_2 (^3B)$	3.87	4.16, 298	3.60, 345	2.58

(n.a. = not available)

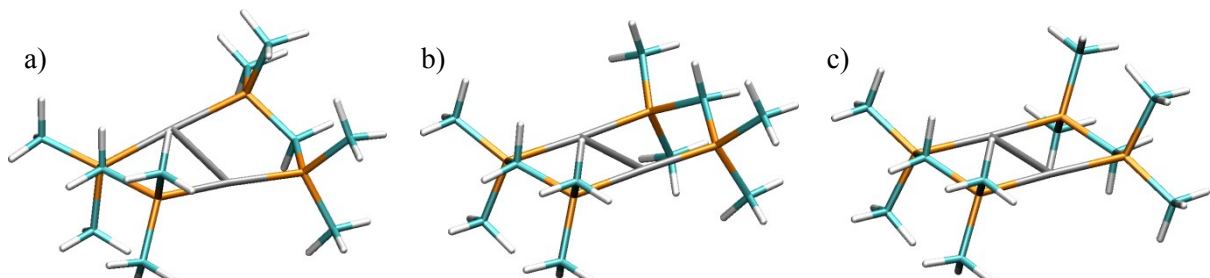


**Fig. S27** Calculated ground state geometries (CC2/def2-TZVPP, capped sticks) of the  $[\text{Ag}_2(\text{dmpm})_2]^{2+}$  model complex for a)  $C_2$  b)  $C_{2v}$  and c)  $C_{2h}$ , conformers, respectively. Color code: Ag (silver), P (yellow), C (cyan), H (white).

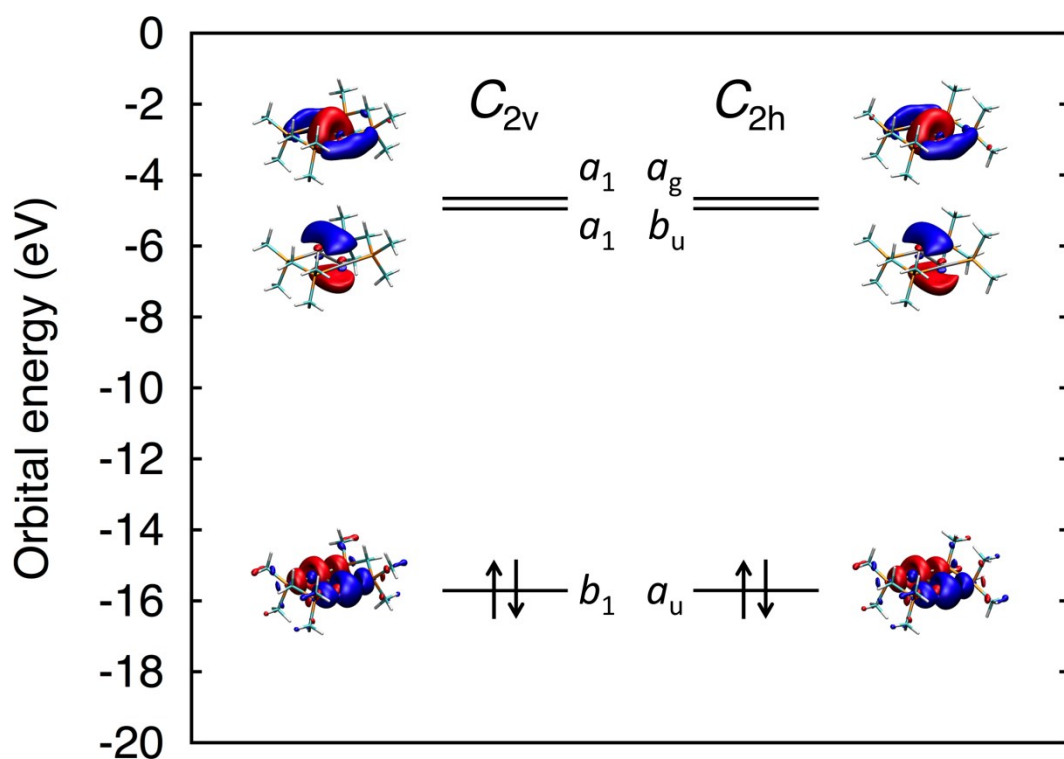
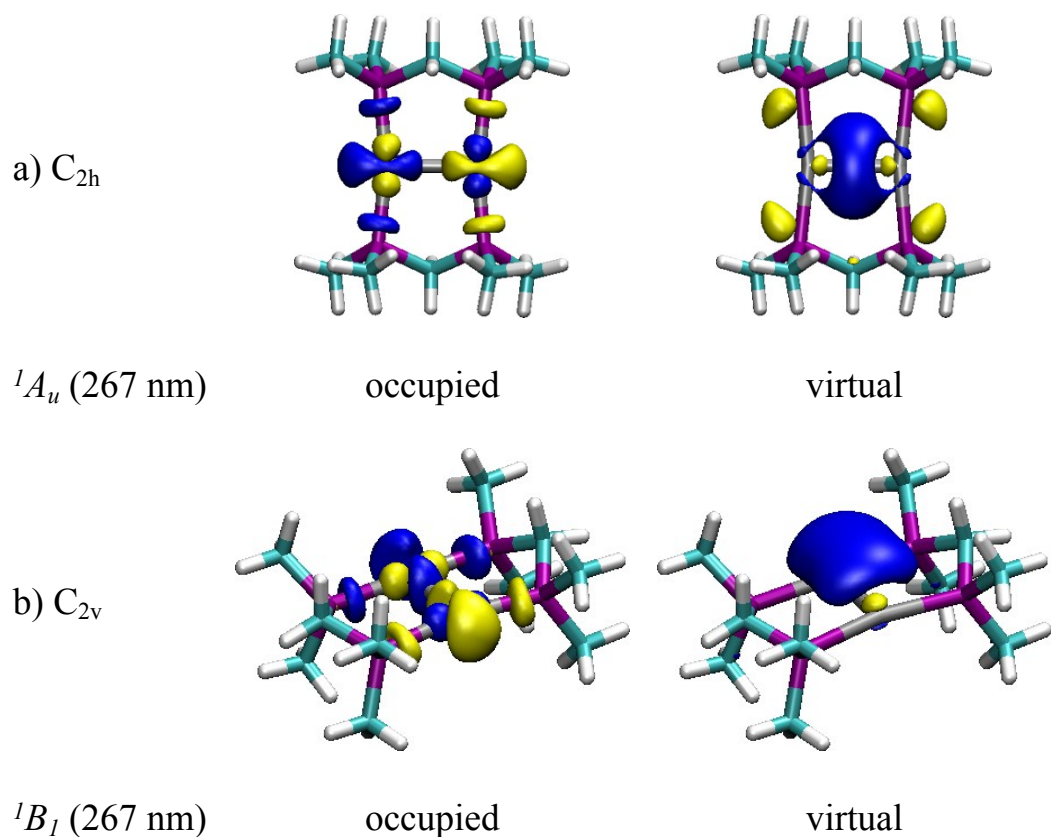


**Fig. S28** MO diagram showing the HOMO, LUMO and LUMO+1 levels (CC2/def2-TZVPP) for structures of the model compound  $[\text{Ag}_2(\text{dmpm})_2]^{2+}$  exhibiting  $C_{2v}$  and  $C_{2h}$  symmetry, respectively. Iso-surface plots at  $\pm 0.04 (a_0)^{-3/2}$  are depicted.

**Fig. S29** Most important occupied and virtual natural transition orbitals (iso-surfaces at  $0.04 (a_0)^{-3/2}$ ) for the  ${}^1\text{MC}(\text{d}\sigma^*-\text{p}\sigma)$  transition at 267 nm for the a)  $C_{2h}$  and b)  $C_{2v}$  isomers of  $[\text{Ag}_2(\text{dmppm})_2]^{2+}$ , respectively (CC2/def2-TZVPP, cf. **Tab. S6**).



**Tab. S7** Cartesian coordinates (in Å) of the optimized structure of  $[\text{Ag}_2(\text{dmpm})_2]^{2+}$  ( $C_{2v}$  isomer,  ${}^1A_1$  ground state) obtained at the CC2/def2-TZVPP level. Ag-Ag stretching frequency  $\nu_{\text{Ag-Ag}} = 84 \text{ cm}^{-1}$ .

44

C	0.000000	3.076343	0.683566
P	1.549341	2.346829	0.036258
Ag	1.469231	0.000000	0.030307
P	1.549341	-2.346829	0.036258
C	0.000000	-3.076343	0.683566
P	-1.549341	-2.346829	0.036258
Ag	-1.469231	0.000000	0.030307
P	-1.549341	2.346829	0.036258
H	0.000000	-4.161839	0.539168
H	0.000000	-2.879049	1.760612
C	-2.832835	-3.080732	1.085087
C	-1.823090	-3.093933	-1.593752
C	-2.832835	3.080732	1.085087
C	2.832835	-3.080732	1.085087
C	1.823090	-3.093933	-1.593752
C	2.832835	3.080732	1.085087
H	0.000000	4.161839	0.539168
H	0.000000	2.879049	1.760612
C	-1.823090	3.093933	-1.593752
C	1.823090	3.093933	-1.593752
H	-2.775653	-4.168829	1.043504
H	-2.709744	-2.747410	2.114073
H	-3.810623	-2.760041	0.727207
H	2.828945	2.833858	-1.923624
H	1.116649	2.711857	-2.326418
H	1.741021	4.179641	-1.531897
H	-3.810623	2.760041	0.727207
H	-2.709744	2.747410	2.114073
H	-2.775653	4.168829	1.043504
H	2.828945	-2.833858	-1.923624
H	1.741021	-4.179641	-1.531897
H	1.116649	-2.711857	-2.326418
H	-1.741021	-4.179641	-1.531897
H	-2.828945	-2.833858	-1.923624
H	-1.116649	-2.711857	-2.326418
H	3.810623	2.760041	0.727207
H	2.775653	4.168829	1.043504
H	2.709744	2.747410	2.114073
H	-2.828945	2.833858	-1.923624
H	-1.741021	4.179641	-1.531897
H	-1.116649	2.711857	-2.326418
H	3.810623	-2.760041	0.727207
H	2.709744	-2.747410	2.114073
H	2.775653	-4.168829	1.043504



**Tab. S8** Cartesian coordinates (in Å) of the optimized structure of  $[\text{Ag}_2(\text{dmpm})_2]^{2+}$  ( $C_{2h}$  isomer,  ${}^1A_g$  ground state) obtained at the CC2/def2-TZVPP level. Ag-Ag stretching frequency  $\nu_{\text{Ag-Ag}} = 84 \text{ cm}^{-1}$ .

44

C	-0.731290	3.058702	0.000000
P	-0.065466	2.345879	-1.549238
Ag	0.000000	0.000000	-1.469424
P	0.065466	-2.345879	-1.549238
C	0.731290	-3.058702	0.000000
P	0.065466	-2.345879	1.549238
Ag	0.000000	0.000000	1.469424
P	-0.065466	2.345879	1.549238
H	-1.803026	2.834379	0.000000
H	-0.614235	4.147479	0.000000
H	0.614235	-4.147479	0.000000
H	1.803026	-2.834379	0.000000
C	1.132421	-3.052823	2.832967
C	-1.545039	-3.134102	1.822824
C	-1.132421	3.052823	2.832967
C	1.545039	3.134102	1.822824
C	1.132421	-3.052823	-2.832967
C	-1.545039	-3.134102	-1.822824
C	-1.132421	3.052823	-2.832967
C	1.545039	3.134102	-1.822824
H	1.118440	-4.141627	2.775912
H	2.152669	-2.693582	2.710062
H	0.766306	-2.741233	3.810649
H	-0.766306	2.741233	-3.810649
H	-2.152669	2.693582	-2.710062
H	-1.118440	4.141627	-2.775912
H	0.766306	-2.741233	-3.810649
H	2.152669	-2.693582	-2.710062
H	1.118440	-4.141627	-2.775912
H	-0.766306	2.741233	3.810649
H	-1.118440	4.141627	2.775912
H	-2.152669	2.693582	2.710062
H	-1.455649	-4.217887	1.740661
H	-1.881413	-2.882509	2.828685
H	-2.287154	-2.770624	1.116446
H	1.881413	2.882509	-2.828685
H	1.455649	4.217887	-1.740661
H	2.287154	2.770624	-1.116446
H	-1.881413	-2.882509	-2.828685
H	-1.455649	-4.217887	-1.740661
H	-2.287154	-2.770624	-1.116446
H	1.881413	2.882509	2.828685
H	2.287154	2.770624	1.116446
H	1.455649	4.217887	1.740661



**Tab. S9** Cartesian coordinates (in Å) of the optimized structure of  $[\text{Ag}_2(\text{dmpm})_2]^{2+}$  ( $C_2$  isomer,  ${}^1A$  ground state) obtained at the CC2/def2-TZVPP level. Ag-Ag stretching frequency  $\nu_{\text{Ag}-\text{Ag}} = 87 \text{ cm}^{-1}$ .

44

C	-0.7023402	3.0569446	0.1606105
P	-0.4719215	2.3019218	-1.4951163
Ag	-0.0000000	0.0000000	-1.3754864
P	0.4719215	-2.3019218	-1.4951163
C	0.7023402	-3.0569446	0.1606105
P	-0.3378375	-2.3195742	1.4733371
Ag	-0.0000000	0.0000000	1.5318191
P	0.3378375	2.3195742	1.4733371
H	-1.7421483	2.8769428	0.4501572
H	-0.5476532	4.1394282	0.1067261
H	0.5476532	-4.1394282	0.1067261
H	1.7421483	-2.8769428	0.4501572
C	0.0769891	-3.2692989	2.9582960
C	-2.0427972	-2.7947224	1.0774245
C	-0.0769891	3.2692989	2.9582960
C	2.0427972	2.7947224	1.0774245
C	1.9996732	-2.7182582	-2.3784705
C	-0.8022985	-3.3010670	-2.3135015
C	-1.9996732	2.7182582	-2.3784705
C	0.8022985	3.3010670	-2.3135015
H	-0.1073568	-4.3307536	2.7907944
H	1.1236574	-3.1165024	3.2162801
H	-0.5415765	-2.9240849	3.7860790
H	-1.9107151	2.3939670	-3.4148284
H	-2.8462630	2.2080637	-1.9224467
H	-2.1648165	3.7958041	-2.3532776
H	1.9107151	-2.3939670	-3.4148284
H	2.8462630	-2.2080637	-1.9224467
H	2.1648165	-3.7958041	-2.3532776
H	0.5415765	2.9240849	3.7860790
H	0.1073568	4.3307536	2.7907944
H	-1.1236574	3.1165024	3.2162801
H	-2.1119161	-3.8700090	0.9080126
H	-2.6812078	-2.5277969	1.9196438
H	-2.3974547	-2.2569134	0.1999133
H	0.8978145	2.9654280	-3.3458063
H	0.5104127	4.3518493	-2.3073172
H	1.7664330	3.1875772	-1.8236628
H	-0.8978145	-2.9654280	-3.3458063
H	-0.5104127	-4.3518493	-2.3073172
H	-1.7664330	-3.1875772	-1.8236628
H	2.6812078	2.5277969	1.9196438
H	2.3974547	2.2569134	0.1999133
H	2.1119161	3.8700090	0.9080126

**Tab. S10** Cartesian coordinates (in Å) of the optimized structure of  $[\text{Ag}_2(\text{dmpm})_2]^{2+}$  ( $C_2$  isomer,  ${}^1B$  singlet excited state ( $S_1$ ) ) obtained at the CC2/def2-TZVPP level.

44

C	-0.5701957	3.1566594	0.1894198
P	-0.6061541	2.2503302	-1.3964078
Ag	0.0000000	0.0000000	-1.2240433
P	0.6061541	-2.2503302	-1.3964078
C	0.5701957	-3.1566594	0.1894198
P	-0.4794609	-2.2754975	1.3903995
Ag	0.0000000	-0.0000000	1.3353792
P	0.4794609	2.2754975	1.3903995
H	-1.5842211	3.1750363	0.5943457
H	-0.2324854	4.1859437	0.0317643
H	0.2324854	-4.1859437	0.0317643
H	1.5842211	-3.1750363	0.5943457
C	-0.1136993	-3.0074777	3.0084039
C	-2.1822378	-2.7715803	1.0266363
C	0.1136993	3.0074777	3.0084039
C	2.1822378	2.7715803	1.0266363
C	2.2656100	-2.5085640	-2.0751553
C	-0.4926635	-3.1643512	-2.5171321
C	-2.2656100	2.5085640	-2.0751553
C	0.4926635	3.1643512	-2.5171321
H	-0.3103980	-4.0805282	2.9742696
H	0.9280353	-2.8348153	3.2723995
H	-0.7563559	-2.5551609	3.7635493
H	-2.3263940	2.0475768	-3.0611512
H	-3.0028090	2.0470019	-1.4213382
H	-2.4624004	3.5786203	-2.1666463
H	2.3263940	-2.0475768	-3.0611512
H	3.0028090	-2.0470019	-1.4213382
H	2.4624004	-3.5786203	-2.1666463
H	0.7563559	2.5551609	3.7635493
H	0.3103980	4.0805282	2.9742696
H	-0.9280353	2.8348153	3.2723995
H	-2.2783524	-3.8567914	1.1011927
H	-2.8485972	-2.2982315	1.7475865
H	-2.4612140	-2.4305529	0.0315966
H	0.4935850	2.6800933	-3.4936055
H	0.1316439	4.1881397	-2.6311329
H	1.5097361	3.1729281	-2.1305904
H	-0.4935850	-2.6800933	-3.4936055
H	-0.1316439	-4.1881397	-2.6311329
H	-1.5097361	-3.1729281	-2.1305904
H	2.8485972	2.2982315	1.7475865
H	2.4612140	2.4305529	0.0315966
H	2.2783524	3.8567914	1.1011927

**Tab. S11** Cartesian coordinates (in Å) of the optimized structure of  $[\text{Ag}_2(\text{dmpm})_2]^{2+}$  ( $C_2$  isomer,  ${}^1A$  singlet excited state ( $S_2$ ) ) obtained at the CC2/def2-TZVPP level.

44

C	-0.7267327	3.0627857	0.0003261
P	-0.0693135	2.3458491	-1.5540469
Ag	0.0000000	0.0000000	-1.3323245
P	0.0693135	-2.3458491	-1.5540469
C	0.7267327	-3.0627857	0.0003261
P	0.0630683	-2.3461241	1.5521190
Ag	0.0000000	0.0000000	1.3317281
P	-0.0630683	2.3461241	1.5521190
H	-1.8008452	2.8459484	0.0025783
H	-0.6003825	4.1512732	-0.0000340
H	0.6003825	-4.1512732	-0.0000340
H	1.8008452	-2.8459484	0.0025783
C	1.0997268	-3.1323131	2.8211722
C	-1.5912195	-3.0587040	1.7732948
C	-1.0997268	3.1323131	2.8211722
C	1.5912195	3.0587040	1.7732948
C	1.1150819	-3.1271594	-2.8186117
C	-1.5815077	-3.0634237	-1.7847107
C	-1.1150819	3.1271594	-2.8186117
C	1.5815077	3.0634237	-1.7847107
H	1.0711926	-4.2176656	2.7055563
H	2.1275610	-2.7850873	2.7267422
H	0.7236181	-2.8623801	3.8068085
H	-0.7426135	2.8581020	-3.8058672
H	-2.1410976	2.7760054	-2.7190653
H	-1.0902656	4.2126842	-2.7037695
H	0.7426135	-2.8581020	-3.8058672
H	2.1410976	-2.7760054	-2.7190653
H	1.0902656	-4.2126842	-2.7037695
H	-0.7236181	2.8623801	3.8068085
H	-1.0711926	4.2176656	2.7055563
H	-2.1275610	2.7850873	2.7267422
H	-1.5665162	-4.1321250	1.5763206
H	-1.9011687	-2.8943488	2.8049620
H	-2.3144001	-2.5831932	1.1147921
H	1.8875440	2.8969191	-2.8171948
H	1.5537723	4.1373723	-1.5909925
H	2.3092864	2.5927048	-1.1278568
H	-1.8875440	-2.8969191	-2.8171948
H	-1.5537723	-4.1373723	-1.5909925
H	-2.3092864	-2.5927048	-1.1278568
H	1.9011687	2.8943488	2.8049620
H	2.3144001	2.5831932	1.1147921
H	1.5665162	4.1321250	1.5763206

**Tab. S12** Cartesian coordinates (in Å) of the optimized structure of  $[\text{Ag}_2(\text{dmpm})_2]^{2+}$  ( $C_2$  isomer,  $^3A$  triplet excited state ( $T_1$ ) ) obtained at the CC2/def2-TZVPP level.

44

C	-0.7268805	3.0682717	0.0236614
P	-0.1327306	2.3222005	-1.5397518
Ag	0.0000000	0.0000000	-1.3192628
P	0.1327306	-2.3222005	-1.5397518
C	0.7268805	-3.0682717	0.0236614
P	0.0031058	-2.3274350	1.5331173
Ag	0.0000000	0.0000000	1.3389808
P	-0.0031058	2.3274350	1.5331173
H	-1.8009005	2.8568468	0.0706650
H	-0.5947888	4.1560349	0.0161701
H	0.5947888	-4.1560349	0.0161701
H	1.8009005	-2.8568468	0.0706650
C	0.9491167	-3.1200087	2.8649033
C	-1.6792475	-2.9864525	1.6861178
C	-0.9491167	3.1200087	2.8649033
C	1.6792475	2.9864525	1.6861178
C	1.2643617	-3.0193481	-2.7762507
C	-1.4796514	-3.0759631	-1.8873932
C	-1.2643617	3.0193481	-2.7762507
C	1.4796514	3.0759631	-1.8873932
H	0.8956669	-4.2057365	2.7651765
H	1.9899676	-2.8031848	2.8192810
H	0.5305984	-2.8231281	3.8253697
H	-0.9272458	2.7317624	-3.7709413
H	-2.2703258	2.6337653	-2.6176450
H	-1.2768084	4.1079963	-2.6972721
H	0.9272458	-2.7317624	-3.7709413
H	2.2703258	-2.6337653	-2.6176450
H	1.2768084	-4.1079963	-2.6972721
H	-0.5305984	2.8231281	3.8253697
H	-0.8956669	4.2057365	2.7651765
H	-1.9899676	2.8031848	2.8192810
H	-1.6748435	-4.0643541	1.5155234
H	-2.0338546	-2.7897956	2.6976047
H	-2.3554439	-2.5061042	0.9832880
H	1.7469871	2.8547995	-2.9202805
H	1.4182652	4.1581844	-1.7600494
H	2.2521833	2.6751144	-1.2360648
H	-1.7469871	-2.8547995	-2.9202805
H	-1.4182652	-4.1581844	-1.7600494
H	-2.2521833	-2.6751144	-1.2360648
H	2.0338546	2.7897956	2.6976047
H	2.3554439	2.5061042	0.9832880
H	1.6748435	4.0643541	1.5155234

**Tab. S13** Cartesian coordinates (in Å) of the optimized structure of  $[\text{Ag}_2(\text{dmpm})_2]^{2+}$  ( $C_2$  isomer,  $^3B$  triplet excited state ( $T_2$ ) ) obtained at the CC2/def2-TZVPP level.

44

C	-0.5709931	3.1487268	0.1923200
P	-0.6095441	2.2450536	-1.3957099
Ag	0.0000000	0.0000000	-1.2357745
P	0.6095441	-2.2450536	-1.3957099
C	0.5709931	-3.1487268	0.1923200
P	-0.4833301	-2.2694164	1.3909234
Ag	-0.0000000	-0.0000000	1.3482856
P	0.4833301	2.2694164	1.3909234
H	-1.5840489	3.1631059	0.6000373
H	-0.2377627	4.1794971	0.0352737
H	0.2377627	-4.1794971	0.0352737
H	1.5840489	-3.1631059	0.6000373
C	-0.1321992	-3.0103798	3.0073355
C	-2.1846058	-2.7587758	1.0105434
C	0.1321992	3.0103798	3.0073355
C	2.1846058	2.7587758	1.0105434
C	2.2719194	-2.5045946	-2.0673951
C	-0.4830143	-3.1658654	-2.5167689
C	-2.2719194	2.5045946	-2.0673951
C	0.4830143	3.1658654	-2.5167689
H	-0.3354394	-4.0819591	2.9668783
H	0.9088753	-2.8452337	3.2783574
H	-0.7764781	-2.5571719	3.7604326
H	-2.3356283	2.0480471	-3.0551693
H	-3.0068279	2.0398143	-1.4132875
H	-2.4696426	3.5749717	-2.1529085
H	2.3356283	-2.0480471	-3.0551693
H	3.0068279	-2.0398143	-1.4132875
H	2.4696426	-3.5749717	-2.1529085
H	0.7764781	2.5571719	3.7604326
H	0.3354394	4.0819591	2.9668783
H	-0.9088753	2.8452337	3.2783574
H	-2.2825531	-3.8445981	1.0731640
H	-2.8550349	-2.2922955	1.7321061
H	-2.4567365	-2.4078752	0.0170430
H	0.4831292	2.6842094	-3.4944269
H	0.1173687	4.1884979	-2.6264599
H	1.5010281	3.1775411	-2.1328981
H	-0.4831292	-2.6842094	-3.4944269
H	-0.1173687	-4.1884979	-2.6264599
H	-1.5010281	-3.1775411	-2.1328981
H	2.8550349	2.2922955	1.7321061
H	2.4567365	2.4078752	0.0170430
H	2.2825531	3.8445981	1.0731640

**Calculated enthalpies / free enthalpies for Cy/(Cy-H) loss of the  $[Ag_2L^{4Me}L^{3Me,Cy}]^{2+}$ ,  $L^{4Me} = (Me_2PCH_2PMc_2) = dmpm$ ,  $L^{3Me,Cy} = (Me_2PCH_2PMcCy)$  model system:**

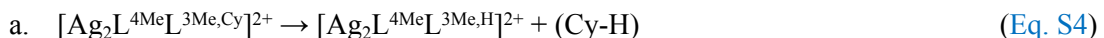
Enthalpies / free enthalpies for homolytic and heterolytic – Cy/(Cy-H) loss dissociation pathways (see Eqs. 3-5) of the  $[Ag_2L^{4Me}L^{3Me,Cy}]^{2+}$  model system ( $L^{4Me} = (Me_2PCH_2PMc_2) = dmpm$ ,  $L^{3Me,Cy} = (Me_2PCH_2PMcCy)$ ) were calculated at the DFT/B3LYP/cc-pVDZ (H, C, N, O), Stuttgart 1997 ECP (Ag) level of theory, respectively. Dissociation enthalpies/free enthalpies were calculated according to  $\Delta_{diss}G/H^{298.15K}(P^{2+} \rightarrow F_1^{2+} + F_2^0) = \Delta_fG/H^{298.15K}(F_1^{2+}) + \Delta_fG/H^{298.15K}(F_2^0) - \Delta_fG/H^{298.15K}(P^{2+})$ , where  $P^{2+}$ : precursor ion,  $F_1^{2+}$ : ionic fragment,  $F_2^0$ : neutral loss fragment.

### 1. Homolytic P-C bond dissociation

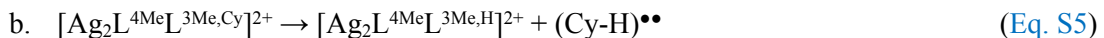


$$\Delta_{diss}G^{298.15K} = 236 \text{ kJ/mol}, \Delta_{diss}H^{298.15K} = 300 \text{ kJ/mol}$$

### 2. Heterolytic P-C bond dissociation and hydrogen transfer



$$\Delta_{diss}G^{298.15K} = 52 \text{ kJ/mol}, \Delta_{diss}H^{298.15K} = 105 \text{ kJ/mol}$$



$$\Delta_{diss}G^{298.15K} = 349 \text{ kJ/mol}, \Delta_{diss}H^{298.15K} = 403 \text{ kJ/mol}$$

**Optimized geometries for the respective  $P^{2+}$ ,  $F_1^{2+}$  and  $F_2^0$  species associated with Eqs. S3-S5 (DFT/B3LYP/cc-pVDZ (H, C, N, O), Stuttgart 1997 ECP (Ag) level of theory using the Gaussian 09 program package, cartesian coordinates are given Å):**

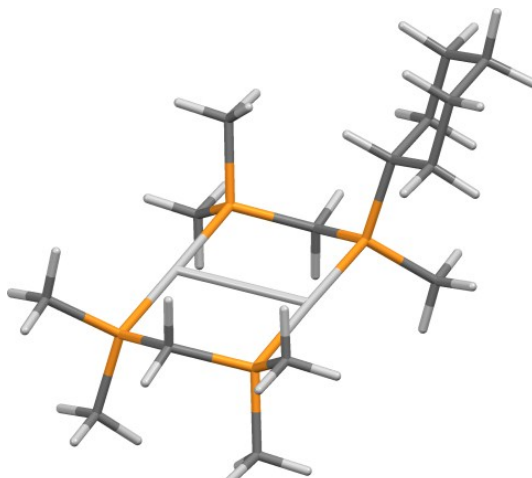
**[Ag<sub>2</sub>L<sup>4Me</sup>L<sup>3Me,Cy</sup>]<sup>2+</sup>**

$\Delta_f H^{298.15K} = -2251.954273$  Hartrees

$\Delta_f G^{298.15K} = -2252.055303$  Hartrees

57

Ag	5.109520	0.865874	9.099100
P	5.901810	-2.921190	7.954680
P	4.383020	-1.201280	10.199500
C	4.460140	-3.771440	7.109820
H	3.633380	-3.041560	7.196940
C	4.760140	-3.964370	5.606050
H	5.633110	-4.631200	5.486670
H	5.029370	-2.999590	5.140030
C	3.553420	-4.581510	4.878200
H	2.716100	-3.859480	4.890200
H	3.812390	-4.742720	3.820030
C	3.109280	-5.895200	5.532460
H	2.218030	-6.289920	5.020740
H	3.901930	-6.655360	5.407570
C	2.818030	-5.702500	7.024920
H	1.943450	-5.037800	7.150380
H	2.550780	-6.661340	7.495800
C	4.024460	-5.097550	7.766450
H	3.770290	-4.949980	8.829390
H	4.861840	-5.816350	7.734810
C	7.265350	-4.160910	8.076750
H	6.946780	-5.041400	8.653670
C	4.472520	-1.169260	12.040300
H	4.159360	-2.138300	12.458600
C	2.642300	-1.690190	9.842070
H	2.471540	-1.769140	8.759130
C	5.448740	-2.663250	9.751320
H	5.003030	-3.584050	10.163700
H	6.406360	-2.503670	10.275600
Ag	6.595530	-0.831619	6.870570
P	5.835030	2.954020	8.036700
P	7.343940	1.242690	5.786510
C	7.283970	3.755090	8.846450
H	8.124360	3.051570	8.928580
C	4.561290	4.283690	7.960260
H	4.960250	5.171970	7.446480
C	7.262860	1.237910	3.944950
H	7.590900	2.207750	3.540250
C	9.087510	1.711420	6.159190
H	9.256380	1.767730	7.243810
C	6.300130	2.721130	6.244200
H	6.774210	3.642180	5.862230
H	5.346950	2.593910	5.703080
H	7.559380	-4.478020	7.065470
H	8.136390	-3.700400	8.565620
H	5.498710	-0.942742	12.364900
H	3.802190	-0.381552	12.416500
H	2.403110	-2.650100	10.325500
H	1.972470	-0.913515	10.241900
H	4.271820	4.559950	8.985500
H	3.669560	3.920100	7.428740
H	6.990560	4.060000	9.862760
H	7.600250	4.647650	8.284430s
H	9.338920	2.677370	5.694140
H	9.751760	0.935458	5.748500
H	6.235480	1.028320	3.612710
H	7.924720	0.446069	3.562460



**[Ag<sub>2</sub>L<sup>4MeL<sup>3Me,H</sup></sup>]<sup>2+</sup>**

$\Delta_f H^{298.15K} = -2017.409112$  Hartrees

$\Delta_f G^{298.15K} = -2017.495295$  Hartrees

41

Ag	-0.017272	-1.627540	0.006702
P	2.424110	1.555600	0.094030
P	2.438840	-1.631720	0.019275
C	3.144410	-0.049447	0.716029
Ag	-0.028151	1.570210	-0.035472
P	-2.471710	-1.621230	-0.007419
P	-2.477310	1.585690	-0.123888
C	-3.188300	-0.041629	-0.697365
H	4.240060	-0.039397	0.587697
H	2.939290	-0.072241	1.799670
H	-4.281630	-0.037767	-0.544692
H	-3.009810	-0.080394	-1.785570
C	-3.247020	-1.859860	1.647410
C	-3.240460	-2.919420	-1.065470
C	-3.290630	1.973400	1.483840
C	-3.202700	2.796670	-1.308120
C	3.219540	-2.930260	1.066480
C	3.213820	-1.842680	-1.639330
C	3.368130	2.056200	-1.409710
H	-2.980880	-2.862570	2.015820
H	-2.871990	-1.119150	2.367610
H	-4.343470	-1.786470	1.576580
H	-2.944050	1.293840	2.275090
H	-3.020820	3.001520	1.770460
H	-4.385690	1.905970	1.389120
H	-4.301610	2.728760	-1.303740
H	-2.903900	3.812100	-1.006460
H	-2.825470	2.604760	-2.323360
H	-2.947190	-3.909010	-0.683219
H	-4.338050	-2.836180	-1.043780
H	-2.884030	-2.822170	-2.101480
H	2.837470	-1.088650	-2.345520
H	4.310290	-1.770310	-1.567810
H	2.947540	-2.838240	-2.026570
H	4.316470	-2.839750	1.041820
H	2.865330	-2.841500	2.104040
H	2.931140	-3.919240	0.678859
H	3.101290	3.096650	-1.650420
H	4.450840	1.996840	-1.225340
H	3.097480	1.420400	-2.264570
H	2.926400	2.451600	1.075800



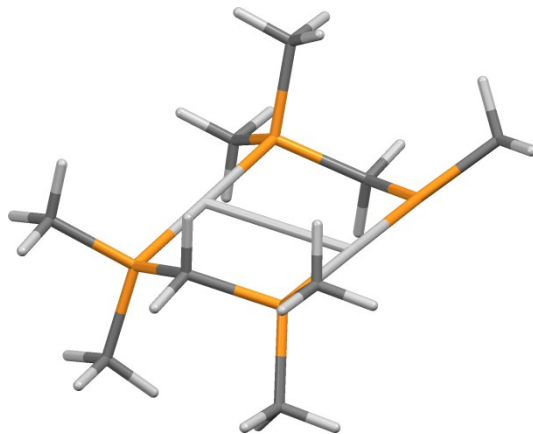
**[Ag<sub>2</sub>L<sup>4Me</sup>L<sup>3Me</sup>]<sup>•2+</sup>**

$\Delta_f H^{298.15K} = -2016.780087$  Hartrees

$\Delta_f G^{298.15K} = -2016.868839$  Hartrees

40

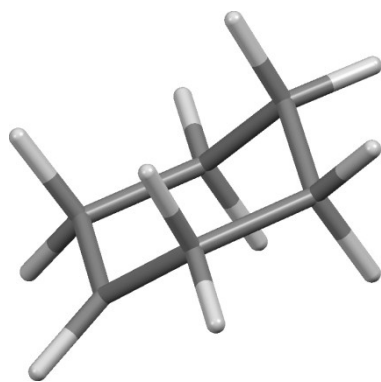
Ag	-0.046521	-1.683740	-0.004840
P	2.363560	1.412480	0.017004
P	2.407720	-1.729900	-0.098431
C	3.158590	-0.162152	0.600515
Ag	-0.069526	1.512780	-0.157256
P	-2.499790	-1.640570	0.084143
P	-2.516040	1.552670	-0.231982
C	-3.234190	-0.107984	-0.688847
H	4.241910	-0.140445	0.397944
H	3.021330	-0.212438	1.695160
H	-4.324020	-0.096105	-0.512611
H	-3.079000	-0.215874	-1.775970
C	-3.201740	-1.749320	1.784650
C	-3.326610	-3.003180	-0.840790
C	-3.317530	2.049800	1.350660
C	-3.237150	2.687320	-1.491150
C	3.229660	-3.069490	0.862482
C	3.098540	-1.865870	-1.800950
C	3.616860	2.339700	-0.954938
H	-2.933940	-2.729020	2.209460
H	-2.782760	-0.967833	2.434190
H	-4.299000	-1.661650	1.757170
H	-2.976710	1.416080	2.181370
H	-3.034930	3.090400	1.572270
H	-4.413410	1.989040	1.261920
H	-4.336450	2.627160	-1.478350
H	-2.930740	3.718200	-1.256980
H	-2.864480	2.427060	-2.492670
H	-3.017210	-3.966210	-0.406952
H	-4.421290	-2.910830	-0.767571
H	-3.024520	-2.979390	-1.898180
H	2.719760	-1.052350	-2.437450
H	4.199020	-1.836310	-1.774630
H	2.778270	-2.824080	-2.237960
H	4.324450	-2.987620	0.780700
H	2.932120	-3.011230	1.919800
H	2.909100	-4.041960	0.458269
H	3.183150	3.295900	-1.280810
H	4.502700	2.536410	-0.329153
H	3.926070	1.758400	-1.840210



**(Cy)<sup>•</sup>** $\Delta_f H^{298.15K} = -235.059887$  Hartrees $\Delta_f G^{298.15K} = -235.096639$  Hartrees

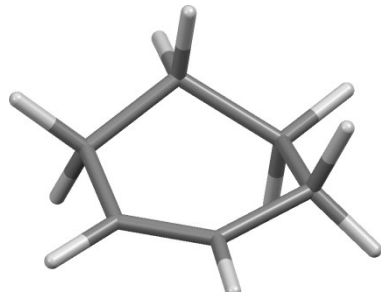
17

C	2.657280	-1.735640	9.804630
H	2.902710	-2.134690	8.792230
C	2.060200	-2.825330	10.639100
H	2.716650	-3.480930	11.218700
C	0.641744	-3.234600	10.392000
H	0.272720	-3.884400	11.203300
H	0.590192	-3.854760	9.466070
C	-0.288517	-2.019200	10.202000
H	-1.287830	-2.355860	9.878040
H	-0.422806	-1.513000	11.175600
C	0.295623	-1.018930	9.195350
H	-0.380385	-0.154187	9.083000
H	0.360523	-1.496740	8.198700
C	1.691280	-0.546850	9.625090
H	1.607530	-0.002592	10.583700
H	2.102090	0.165734	8.889920
H	3.617290	-1.396150	10.228600

**(Cy-H)** $\Delta_f H^{298.15K} = -234.505110$  Hartrees $\Delta_f G^{298.15K} = -234.540228$  Hartrees

16

C	2.518070	-1.754150	9.932890
H	3.601250	-1.589800	9.943630
C	2.030840	-2.948360	10.296300
H	2.724280	-3.748570	10.577800
C	0.555809	-3.265800	10.344200
H	0.327313	-3.832510	11.264500
H	0.302752	-3.950870	9.510670
C	-0.310513	-1.999630	10.269700
H	-1.362330	-2.268100	10.076500
H	-0.289294	-1.487350	11.249100
C	0.210638	-1.040220	9.192710
H	-0.447691	-0.160185	9.103670
H	0.188576	-1.552030	8.213000
C	1.649350	-0.598410	9.499290
H	1.649540	0.176117	10.291900
H	2.095760	-0.108611	8.615470



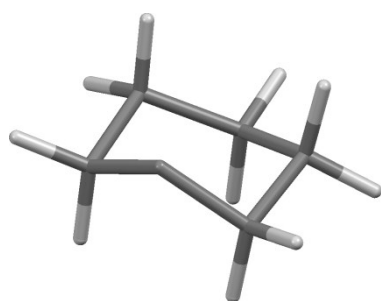
**(Cy-H)<sup>••</sup>**

$\Delta_f H^{298.15K} = -234.391541$  Hartrees

$\Delta_f G^{298.15K} = -234.426920$  Hartrees

16

C	2.620880	-1.793180	9.859790
H	2.693420	-2.345510	8.897600
C	1.916970	-2.506230	10.953100
C	0.726975	-3.206150	10.412300
H	0.282705	-3.921480	11.122700
H	0.869680	-3.703510	9.428300
C	-0.283416	-2.016820	10.197800
H	-1.238280	-2.441770	9.849600
H	-0.477980	-1.530120	11.167800
C	0.283095	-0.998665	9.204140
H	-0.388021	-0.125089	9.135250
H	0.323999	-1.449030	8.196370
C	1.686230	-0.548941	9.621670
H	1.631920	0.043877	10.549800
H	2.157070	0.088014	8.856030
H	3.620450	-1.432170	10.149900



## **References:**

- [1] A. Zavras, A. Ariafard, G. N. Khairallah, J. M. White, R. J. Mulder, A. J. Carty, R. A. J. O'Hair *Nanoscale*. **2015**, 7, 18129-18137. doi: 10.1039/C5NR05690J
- [2] A. Zavras, G. N. Khairallah, M. Krstić, M. Girod, S. Daly, R. Antoine, P. Maitre, R. J. Mulder, S.-A. Alexander, V. Bonačić-Koutecký, P. Dugourd, R. A. J. O'Hair *Nature Communications*. **2016**, 7, 11746. doi: 10.1038/ncomms11746
- [3] A. J. Clark, A. Zavras, G. N. Khairallah, R. A. J. O'Hair *International Journal of Mass Spectrometry*. **2015**, 378, 86-94. doi: <https://doi.org/10.1016/j.ijms.2014.07.015>
- [4] A. Zavras, M. Krstić, P. Dugourd, V. Bonačić-Koutecký, R. A. J. O'Hair *ChemCatChem*. **2017**, 9, 1298-1302. doi: 10.1002/cctc.201601675